

IMPLEMENTATION OF FRACTIONAL ORDER VISCOELASTIC MODELS TO
FINITE ELEMENT METHOD

A THESIS SUBMITTED TO
THE GRADUATE SCHOOL OF NATURAL AND APPLIED SCIENCES
OF
MIDDLE EAST TECHNICAL UNIVERSITY

BY

PARNIAN HESAMMOKRI

IN PARTIAL FULFILLMENT OF THE REQUIREMENTS
FOR
THE DEGREE OF MASTER OF SCIENCE
IN
MECHANICAL ENGINEERING

SEPTEMBER 2019

Approval of the thesis:

**IMPLEMENTATION OF FRACTIONAL ORDER VISCOELASTIC
MODELS TO FINITE ELEMENT METHOD**

submitted by **PARNIAN HESAMMOKRI** in partial fulfillment of the requirements
for the degree of **Master of Science in Mechanical Engineering Department,
Middle East Technical University** by,

Prof. Dr. Halil Kalıpçılar
Dean, Graduate School of **Natural and Applied Sciences** _____

Prof. Dr. M. A. Sahir Arıkan
Head of Department, **Mechanical Engineering** _____

Assoc. Prof. Dr. Ergin Tönük
Supervisor, **Mechanical Engineering, METU** _____

Examining Committee Members:

Prof. Dr. F. Suat Kadiođlu
Mechanical Engineering Department, METU _____

Assoc. Prof. Dr. Ergin Tönük
Mechanical Engineering, METU _____

Assoc. Prof. Dr. Mehmet Bülent Özer
Mechanical Engineering Department, METU _____

Assist. Prof. Dr. Orkun Özşahin
Mechanical Engineering Department, METU _____

Assist. Prof. Dr. Bilsay Sümer
Mechanical Engineering Department, Hacettepe University _____

Date: 11.09.2019

I hereby declare that all information in this document has been obtained and presented in accordance with academic rules and ethical conduct. I also declare that, as required by these rules and conduct, I have fully cited and referenced all material and results that are not original to this work.

Name, Surname: Parnian Hesammokri

Signature:

ABSTRACT

IMPLEMENTATION OF FRACTIONAL ORDER VISCOELASTIC MODELS TO FINITE ELEMENT METHOD

Hesammokri, Parnian
Master of Science, Mechanical Engineering
Supervisor: Assoc. Prof. Dr. Ergin Tönük

September 2019, 83 pages

In the latest decades, fractional calculus has been commonly used to define the behavior of viscoelastic materials. Real viscoelastic materials such as rubbers, polymers, soft biological tissues, asphalt mixtures, soils, etc. represent power law creep and relaxation behaviors. In Scientific literature relaxation and creep of this type of material has been modelled, primarily through single and/or linear combinations of exponential functions, in an effort to capture the contributions of both solid and fluid phases. This strategy does not allow experimental findings to fit correctly. In this study, isotropic 3-D constitutive equations are evaluated using the fractional calculus by means of the concept of fading memory for a single spring pot, the fractional Kelvin-Voigt model, and the fractional standard linear solid model to reproduce the actual behavior of these materials. Using the UMAT subroutine in ABAQUS / Standard, a finite element code is developed for each model. To reach the strain and stress history of all fractional models, the Boltzmann superposition concept and the fractional derivatives evaluated by Grünwald-Letnikov were used. Relaxation and creep responses have been obtained for each fractional model and these computational results are compared to analytical results to demonstrate the correctness of the finite element codes. Access to the history of strain and stress at each Gauss point of each component is essential for the implementation of the model in a constructive way

which is one of the most important aims of this study which has been reached by developing the finite element code using the Jacobian matrix not the strain energy density function which utilized widely in literature. These codes can describe the transition of the viscoelastic models' behavior smoothly from rubbery to glassy just by changing the fractional coefficients.

It has been shown that using this technique the process of extracting material parameters can be much easier as less coefficients are required compared to other techniques in constitutive models. This study demonstrates that 3D fractional viscoelastic models can be readily and effectively implemented in finite element software.

Keywords: Fractional Calculus, Viscoelasticity, Finite Element Method

ÖZ

TAMSAYI OLMAYAN TÜREVLİ VISKOELASTİK MODELLERİN SONLU ELEMANLAR ANALİZİNE UYGULAMASI

Hesammokri, Parnian
Yüksek Lisans, Makina Mühendisliği
Tez Danışmanı: Doç. Dr. Ergin Tönük

Eylül 2019, 83 sayfa

Son yıllarda, viskoelastik malzemelerin davranışını tanımlamak için fraksiyonel analiz yaygın olarak kullanılmıştır. Kauçuklar, polimerler, yumuşak biyolojik dokular, asfalt karışımları, topraklar vb. gibi gerçek viskoelastik malzemeler, güç yasaasının gevşeme ve sünme davranışlarını temsil eder. Bilimsel literatürde, bu tür materyalin gevşeme ve sünmesi, hem katı hem de sıvı fazların etkilerini gözlemek amacıyla, öncelikle üstel fonksiyonların tekli ve / veya doğrusal kombinasyonları yoluyla modellenmiştir. Fakat bu strateji, deneysel bulgulara uygun değildir. Bu çalışmada üç boyutlu eşyönlü bünye denklemleri sönümlü bellek yaklaşımı ile tek bir *spring-pot*, tamsayı türevli olmayan Kelvin-Voigt modeli ve standart doğrusal katı modeli ile gerçek malzemelerin mekanik yanıtını modellemek için kullanılmıştır. ABAQUS/Standart sonlu elemanlar yazılımındaki UMAT altprogramı ile, her bir model için sonlu elemanlar modelleri elde edilmiştir. Modellerdeki gerinme ve gerilme tarihçelerini elde etmek için Boltzmann üstdüşüm özelliği ve tamsayı olmayan türevler için de Grünwald-Letnikov yöntemi kullanılmıştır. Gevşeme ve sünme yanıtları elde edilerek analitik sonuçlarla karşılaştırılmıştır. Her bileşenin her Gauss noktasındaki gerilme ve gerinme geçmişine erişim, literatürde yaygın olarak kullanılmakta olan gerilme enerji yoğunluğu işlevi yerine Jacobian matrisi kullanılarak sonlu element kodlarının elde edilmesiyle geliştirilen modelin,

çalıřmanın en temel amalarından biri olan yapısal bir biçimde uygulanabilmesi esastır. Bu kodlar viskoelastik modellerin davranıřlarının kauuktan camsıya sadece kesirli katsayıları deęiřtirerek geiřini aıklayabilir. Bu yolla sayısı daha az olan malzeme parametrelerinin eldesinin daha kolay olacaęı gsterilmiřtir. Bu alıřma ile  boyutlu tam sayı olmayan trevli malzeme modellerinin solu elemanlar teknięine uygulanabileceęi gsterilmiřtir. Geliřtirilen sonlu elemanlar analiz yntemi viskoelastik malzemelerle ilgili arařtırma, deney ve tasarım srelerinde kullanılabilir.

Anahtar Kelimeler: Kesirli Analiz, Viscoelastisite, Sonlu Elemanlar Metodu

To the best friends ever, Mommy and Daddy...

ACKNOWLEDGEMENTS

Firstly, I would like to express my sincere gratitude to my advisor Associate Prof. Dr. Ergin Tönük for the continuous support of my M.Sc. study and related research, for his patience, motivation, and immense knowledge. His guidance helped me in all the time of research and writing of this thesis. I could not have imagined having a better advisor and mentor for my M.Sc. study.

I would like to thank my family, my parents who have supported me in any situation. I am using this opportunity to express my gratitude to everyone who supported me during this period, especially my dear friends Tannaz Mohammadi, Melika Mohsenizade, Mahsa Monirizad, Iman Ehsandar, and Sevim Seda Çokoğlu. This thesis would not be completed without their unlimited patronage.

I am also grateful to Mr. Ramin Rouzbar for sharing his truthful and enlightening views on some thesis issues.

TABLE OF CONTENTS

ABSTRACT	v
ÖZ	vii
ACKNOWLEDGEMENTS	x
TABLE OF CONTENTS	xi
LIST OF TABLES	xiv
LIST OF FIGURES	xv
CHAPTERS	
1. INTRODUCTION	1
1.1. Motivation	1
1.2. Problem Definition	4
1.3. Thesis Outline.....	5
2. LITERATURE REVIEW	7
2.1. Linear Theory of Elasticity.....	7
2.2. Non-Linear Theory of Elasticity	9
2.3. Linear Theory of Viscoelasticity	9
2.3.1. The Linear Elastic Solid (The Linear Spring)	11
2.3.2. The Linear Viscous Fluid (The Linear Dashpot).....	11
2.4. Introduction to Fractional Calculus.....	14
2.4.1. The Gamma Function	14
2.4.2. Laplace Transform and Convolution	15
2.4.3. The Mittag-Leffler Function.....	15
2.4.4. Grünwald-Letkinov and Riemann-Liouville Fractional Operators	16

2.4.5. Caputo Fractional Operator	18
2.5. Fractional Calculus in the Theory of Viscoelasticity	18
2.6. The Quasi-Linear Viscoelastic Theory (QLV)	25
2.7. The Fractional Order Viscoelastic Model (FOV)	27
2.8. Implementing Viscoelastic Models Using Strain Energy Density Function ..	29
2.9. Implementing Viscoelastic Models Using Boltzmann Superposition	34
3. METHODOLOGY	37
3.1. Grünwald Coefficient.....	37
3.2. Generalizing a 3-D Isotropic Constitutive Law for a FKV Model	40
3.3. Numerical Evaluation of the Constitutive Model of FKV	42
3.3.1. Normal Stresses	42
3.3.2. Shear Stresses	44
3.4. Finite Element Implementation.....	44
3.4.1. UMAT Subroutine.....	44
3.4.1.1. Steps Required in Writing a UMAT	44
3.5. Developing a UMAT Subroutine for FKV Model.....	45
3.6. Developing a UMAT Subroutine for Fractional Standard Linear Solid Model	50
4. RESULTS AND DISCUSSION	55
4.1. Fractional Kelvin-Voigt (FKV)Model.....	55
4.1.1. Analytical Solution.....	56
4.1.2. Computational Results	57
4.2. Single Fractional Element (Spring-Pot).....	61
4.3. Fractional Standard Linear Solid Model.....	64

4.3.1. Analytical Solution	64
4.3.2. Computational Results.....	65
5. CONCLUSION AND RECOMMENDATIONS FOR FUTURE STUDIES	75
5.1. Conclusion and Discussion	75
5.2. Future Studies.....	76
REFERENCES.....	79

LIST OF TABLES

TABLES

Table 4.1. Material parameters which used for fractional Kelvin-Voigt model (Alotta et al., 2018).	56
Table 4.2. Material parameters used for fractional standard linear solid model (Alotta et al., 2018).	65

LIST OF FIGURES

FIGURES

Figure 1.1. Fractional models (a) spring-pot (b) fractional Kelvin-Voigt (c) fractional Maxwell (d) fractional standard linear solid 1 (f) fractional standard linear solid 2 (Alotta et al., 2018).	3
Figure 2.1. Creep test on a linear viscoelastic material (Lakes, 1998).	10
Figure 2.2. Relaxation test on a linear viscoelastic material (Lakes, 1998).....	10
Figure 2.3. A linear spring (Lakes, 1998).	11
Figure 2.4. An ideal incompressible viscous fluid limited by a movable upper disk and a fixed lower disk (Lakes, 1998).....	12
Figure 2.5. A linear dashpot (Lakes, 1998).....	12
Figure 2.6. Classical viscoelastic material models. (Larrabee and Wayne, 1986).....	13
Figure 2.7. Sequential realization of the frictional element (Schiessel et al., 1995)..	22
Figure 2.8. (a) elastic, (b) viscous and (c) fractional element (Schiessel et al., 1995).	23
Figure 2.9. Unlimited number of series-connected standard linear solid models (Fung, 1993).	26
Figure 2.10. QLV (serial) and FOV (fractional) model spring and dashpot representations. (a) FOV may be depicted with a fractal tree model (b) varying in width and depth based on the fractional order φ (Doehring et al., 2005).....	28
Figure 2.11. A generalized linear Kelvin-Voigt material model (Tonuk and Silver-Thorn, 2004).....	31
Figure 2.12. The Generalized Maxwell Model (Fukunaga and Shimizu, 2015).....	34
Figure 3.1. Fractional Kelvin-Voigt (FKV) model.	40
Figure 3.2. Flow chart for the Jacobian matrix.	49
Figure 3.3. Flow chart for the strain history matrix.	50
Figure 3.4. Fractional Standard Linear Solid Model.....	50

Figure 4.1. The single element in the ABAQUS software. 55

Figure 4.2. Strain history during the relaxation test (the strain in the curve is ϵ_{11}). 57

Figure 4.3. Comparison between analytical and computational results for the relaxation test for the fractional Kelvin-Voigt model (the stress in the curve is σ_{11}).
..... 58

Figure 4.4. Different behavior of the fractional Kelvin-Voigt model for relaxation test for different values of fractional coefficient (the stress in the curve is σ_{11}). 59

Figure 4.5. Stress history during the creep test (the stress in the curve is σ_{11}). 59

Figure 4.6. Different behavior of the fractional Kelvin-Voigt model for creep test for different values of fractional coefficient (the strain in the curve is ϵ_{11}). 60

Figure 4.7. Different behavior of the fractional Kelvin-Voigt model for creep test for different values of fractional coefficient (the strain in the curve is $\epsilon_{22} = \epsilon_{33}$). 60

Figure 4.8. Different behavior of the single spring-pot for the relaxation test for different values of fractional coefficient (the stress in the curve is σ_{11}). 62

Figure 4.9. Different behavior of the single spring-pot for creep test for different values of fractional coefficient (the strain in the curve is ϵ_{11}). 63

Figure 4.10. Different behavior of the single spring-pot for creep test for different values of fractional coefficient (the strain in the curve is $\epsilon_{22} = \epsilon_{33}$). 63

Figure 4.11. Comparison between analytical and computational results for the relaxation test for the fractional standard linear solid model (the stress in the curve is σ_{11}). 66

Figure 4.12. Different behavior of the fractional standard linear solid model for the relaxation test for different values of fractional coefficient (the stress in the curve is σ_{11}). 66

Figure 4.13. Different behavior of the fractional standard linear solid model for creep test for different values of fractional coefficient (the strain in the curve is ϵ_{11}). 67

Figure 4.14. Different behavior of the fractional standard linear solid model for creep test for different values of fractional coefficient (the strain in the curve is $\epsilon_{22} = \epsilon_{33}$).
..... 67

Figure 4.15. Strain history during the relaxation test (the strain in the curve is ϵ_{11}).	68
Figure 4.16. Stress history during the creep test (the stress in the curve is σ_{11}).	69
Figure 4.17. Different behavior of the fractional Kelvin-Voigt model for the relaxation test for different values of fractional coefficient (the stress in the curve is σ_{11}).	69
Figure 4.18. Different behavior of the fractional standard linear solid model for the relaxation test for different values of fractional coefficient (the stress in the curve is σ_{11}).....	70
Figure 4.19. Different behavior of the fractional Kelvin-Voigt model for creep test for different values of fractional coefficient (the strain in the curve is ϵ_{11}).....	70
Figure 4.20. Different behavior of the fractional Kelvin-Voigt model for creep test for different values of fractional coefficient (the strain in the curve is $\epsilon_{22} = \epsilon_{33}$)..	71
Figure 4.21. Different behavior of the fractional standard linear solid model for creep test for different values of fractional coefficient (the strain in the curve is ϵ_{11}).....	71
Figure 4.22. Different behavior of the fractional standard linear solid model for creep test for different values of fractional coefficient (the strain in the curve is $\epsilon_{22} = \epsilon_{33}$).	72

CHAPTER 1

INTRODUCTION

1.1. Motivation

In particular, materials such as polymers demonstrate behaviors which depends on time, like creep, relaxation, and damping. Classical viscoelastic designs often involve multiple parameters to properly portray the behavior of these materials. Many of the related research focuses first on formulating credible constitutive equations and then on solving boundary or initial value problems. It is not possible to carry out the analyzes without a proper constitutive equation and boundary and initial value problems cannot be solved. Therefore, it is extremely essential to formulate suitable constitutive relationships to agree well with the test outcomes. A considerable issue is the selection of the suitable model to fit the test outcomes. To correlate with the experimental information, these models should match all results of the experiment including relaxation, creep, hysteresis ... etc. Implementing the material model to a finite element subroutine numerically is one of the most significant results of the expanding of a viscoelastic model.

The finite element approach is one of the most effective tools to study the numerical solution of viscoelastic problems and it is possible to simulate and solve real-world problems with the advancement of computer technology. Classical viscoelastic models often involve multiple constants to reproduce the material's real behavior. To model a viscoelastic material accessing the strain or stress history is one of the issues which cannot be fulfilled using the classical viscoelastic material models. Also in these models the extraction of material parameters is another issue regarding the high number of parameters. In this regard, constitutive equations using non-integer derivatives have the privilege of involving fewer parameters and the availability of strain or stress history. By using fractional derivative an additional parameter to be

identified is the non-integer derivative parameter that is the order of time derivative of stress and/or strains in the constitutive equation, which can replace many other constants in integer-order models by simplifying the material model. Identifying these material parameters needs to cope with difficult mathematics which is much more challenging if it be compared to the integer-order models. Several numerical algorithms are proposed in the literature to address the differentiation of non-integer order and integration for models of those materials. Since one of the purposes of evaluating constitutive equations for viscoelastic materials is identifying constants of the material model generated through curve-fitting to the test results utilizing the inverse finite element approach, the model should fit the test outcomes well with a small but sufficient number of constants. Another benefit in the using of the non-integer derivatives is the inclusion of memory conduct by definition in non-integer operators that is unique to viscoelastic materials. Viscoelastic materials have memory and the fractional calculus used in the theory of viscoelasticity is the memory imitation (Schiessel et al., 1995).

Only one fractional derivative operator is required for the most ordinary viscoelastic uniaxial fractional-order model that acts on stress and strain. For some polymers, only four constants are needed. Among those parameters two of them is "elastic" parameters, one is the relaxation time constant and the other one is the non-dimensional non-integer order of differentiation, which the comparison of it with experimental results is in a good agreement (Welch et al., 1999; Bagley and Torvik 1983).

Researchers have been interested in using fractional viscoelastic models over the past decades as they are able to correctly portray both the creep and relaxation behavior of viscoelastic materials and the experimentally captured "fading" memory impacts. It is commonly demonstrated that the stress-strain relation of viscoelastic materials during a creep or relaxation experiment can be shown by power law which depends on time; examples include polymers, soft biological tissues, soil etc. In creep and relaxation a power law contributes to non-integer viscoelastic constitutive laws defined by the existence of non-integer order derivatives and integrals. The most appealing element

in the fractional viscoelastic constitutive models is that the stress-strain response depends on the prior stress-strain history, which enables consideration of the material's long "fading" memory. The hereditary theory is one of the bases of the linear viscoelasticity. Boltzmann (1876) developed a concept for the first time which uses an essential relationship of convolution between stress and strain. Using the concept of Boltzmann superposition, the hereditary theory of linear viscoelasticity developed, in this theory the present stress is calculated by the superposing of stress reactions to the whole strains.

Non-integer derivatives are dependent on the material past, evidencing a mechanism of memory, and incorporating the history of a process inherently. Furthermore, the non-integer order parameter offers a smooth transition from elastic to Newtonian viscous behavior by defining a fractional coefficient which changes between zero and one (Alotta et al., 2018). Furthermore, it is possible to understand fractional relationships of viscoelastic components physically using hierarchical formations of dashpots and springs, in the concept of fractional calculus the dashpot will be replaced by a new element called spring-pot which is also called fractional element, then the fractional viscoelastic models will be generated (figure 1.1). The reasons listed above are the primary motivations in characterizing the viscoelastic behavior by using the fractional calculus.

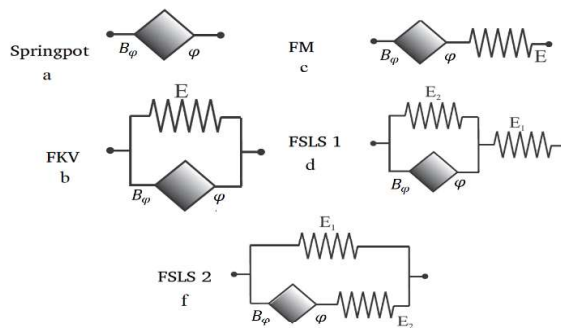


Figure 1.1. Fractional models (a) spring-pot (b) fractional Kelvin-Voigt (c) fractional Maxwell (d) fractional standard linear solid 1 (f) fractional standard linear solid 2 (Alotta et al., 2018).

1.2. Problem Definition

To utilize these models to depict the behavior of complicated real materials, the application of these constitutive models into FE packages is essential. In the literature the number of people who have tried to implement fractional 3-D constitutive models into FE software is very low. Among the people who did their best to implement these models in an accurate way into finite element code Enelund et al. in 1999, Demirci and Tonuk in 2011 and Alotta et al, in 2018 can be mentioned. In 1999 Enelund et al. proposed a physically sound formulation for a set of internal variables for the standard linear solid model with integer and non-integer order rate equations. Using the Generalized Midpoint law a time integration method is utilized to integrate the constitutive response. Demirci and Tonuk developed their model using strain energy function and they did their analysis in MSC MARC software. In 2018 Alotta et al., developed fractional constitutive laws for most of the models but they did not report any results regarding fractional standard linear solid model for the case which the spring is in parallel with the fractional Maxwell model (figure 1.1 (f)). they developed their code in Fortran and used both ABAQUS Implicit and Explicit.

In this study fractional 3-D constitutive models are evaluated using the concept of fading memory to obtain the real behavior of viscoelastic models for a single spring pot (figure 1.1 (a)), the fractional Kelvin-Voigt model (figure 1.1 (b)), and the fractional standard linear solid model (figure 1.1 (f)). Stress history and strain history for each model at each Gauss point of each component obtained and stored in column matrices during the simulation which can be reached easily to implement the model in a constructive method. Accessibility to these histories became possible by utilizing the Boltzmann superposition theory and the Jacobian matrix for each instant of time which is completely different from methods which used strain energy function to develop their finite element codes.

1.3. Thesis Outline

The constitutive models for a single spring pot (figure 1.1 (a)), the fractional Kelvin-Voigt model (figure 1.1 (b)), and the fractional standard linear solid model (figure 1.1 (f)) have been expanded to implement in finite element code and by comparing the computational results with the analytical outcomes their applicability to reproduce the response of linear viscoelastic materials have been shown. The finite element codes have been written using UMAT subroutine which is one of the routines for ABAQUS/Standard, more details about this subroutine can be found in chapter 3. The major difference between this work and most of the works which have been done up to now is using the Jacobian matrix instead of the strain energy function which requires different series of steps.

In the next chapter a literature review has been presented including fractional calculus theory and its application in the theory of viscoelasticity and the methods which have been offered by other researchers through this way like generating constitutive models for viscoelastic materials and finite element approaches. In the third chapter, the methodology which has been used in this study explained in detail including both the procedure which is taken to expand the constitutive equations to be used in finite element code and the numerical method which made this approach computationally efficient. In Chapter 4, the results for analytical and computational methods are presented and those outcomes were compared with each other and a discussion is done based on what has been obtained. The last chapter contains the conclusion and suggestions for future studies.

CHAPTER 2

LITERATURE REVIEW

2.1. Linear Theory of Elasticity

A material can be considered as linearly elastic or Hookean as long as the force required to stretch or compress it is proportional to that distance (Timoshenko, 1983). By doing the tensile testing (uniaxial loading) on a specimen the longitudinal stress on a small element of the sample can be calculated as:

$$\sigma = \frac{F}{A} \quad (2.1)$$

In the equation above A is the instantaneous cross sectional area. By replacing A_i which is the cross sectional area for the initial state in the equation above, the engineering stress (σ_e) will be obtained:

$$\varepsilon = \int_{l_i}^l \frac{dl}{l} = \ln\left(\frac{l}{l_i}\right) \quad (2.2)$$

and the engineering strain is:

$$\varepsilon_e = \int_{l_i}^l \frac{dl}{l_i} = \frac{l - l_i}{l_i} \quad (2.3)$$

Just like true and engineering stresses in the elastic domain the engineering and true strains are approximately equal at this regime (infinitesimal strain).

At the tension test the theory of linear elasticity can be well described by Hook's law:

$$\sigma = E\varepsilon \quad (2.4)$$

where E is the Young's (elastic) modulus. Physical constants can be obtained from easy studies completely characterize the mechanical response of a linearly elastic body. Test such as uniaxial tension or uniaxial compression, for example, produces both the Young's modulus and the Poisson's ratio. From these two constants, any other linear elastic constant can be acquired. In many engineering applications, the hypothesis that materials are linearly elastic under the small strain regime with potentially a geometrically nonlinear behavior is used effectively (Love, 2013).

Based on generalized Hooke's law at the domain of linear elasticity the stress components are linear homogenous functions of the strain components.

$$\sigma_{ij} = D_{ijkl}\varepsilon_{kl} \quad i, j = 1, 2, 3, \quad \text{suumation convention applies} \quad (2.5)$$

D_{ijkl} is a tensor which represents the elastic parameters. Using equation above the elastic strain energy W per unit volume has been defined:

$$W = \frac{1}{2}\sigma_{ij}\varepsilon_{kl} = \frac{1}{2}D_{ijkl}\varepsilon_{ij}\varepsilon_{kl} \quad (2.6)$$

$$\sigma_{ij} = \frac{\partial W}{\partial \varepsilon_{ij}} \quad (2.5)$$

For the isotropic linear elastic materials the stress-strain relationship is:

$$\sigma_{ij} = \lambda\varepsilon_{kk}\delta_{ij} + 2G\varepsilon_{ij} \quad (2.8)$$

δ_{ij} is the Kronecker, and λ is the Lamé's constant and G is the shear modulus.

For small displacement stain can be determined as below neglecting the higher order term (Sadd, 2004):

$$\varepsilon_{ij} = \frac{1}{2}\left(\frac{\partial u_i}{\partial x_j} + \frac{\partial u_j}{\partial x_i}\right) \quad (2.9)$$

2.2. Non-Linear Theory of Elasticity

Most of the materials require finite deformations where these deformations are nonlinear and the related stresses rely on the material characteristics underlying them. Generally speaking, it is not possible to represent the mechanical behaviors of non-linear elastic materials using constants, but are defined by parameters that are scalar deformation functions (Mihai and Goriely, 2017). By considering a 3-D body in a domain $\Omega \subset \mathbb{R}^3$ that is subjected to a finite strain and denoting its transformation as \mathbf{x} , and by assuming \mathbf{X} as the Lagrangian (reference configuration) and \mathbf{x} as the Eulerian (current configuration) coordinates The deformation gradient will be:

$$\mathbf{F} = \text{Grad}\mathbf{x}(\mathbf{X}) \quad (2.10)$$

$$J = \det\mathbf{F} > 0 \quad (2.6)$$

The displacement of a material point is:

$$\mathbf{u}(\mathbf{X}) = \mathbf{x} - \mathbf{X} \quad (2.7)$$

$$\nabla\mathbf{u} = \text{Grad}\mathbf{u} = \mathbf{F} - \mathbf{I} \quad (2.8)$$

\mathbf{I} , is the identity tensor (Ogden, 1997; Biot, 1965).

2.3. Linear Theory of Viscoelasticity

The relationship between strain and stress is time-dependent for a viscoelastic material. The theory of linear viscoelasticity implies that the time-dependent behavior is independent of strain (i.e. strain energy density can be broken down into an instantaneous/glassy part (which can be nonlinear) and a time-dependent part as a product). Figure 2.1 shows a creep test which demonstrates the typical behavior of a viscoelastic material to a steady load and removal of it which involves elastic and permanent plastic strains, and over time the strain rises. This time-dependent reaction is referred to as creep.

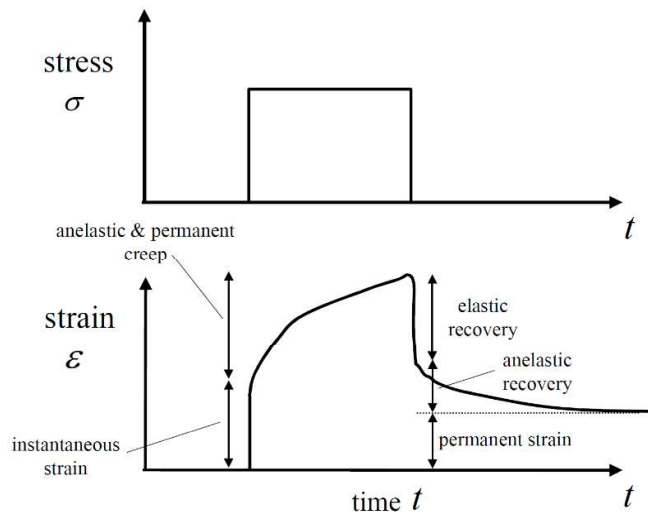


Figure 2.1. Creep test on a linear viscoelastic material (Lakes, 1998).

Figure 2.2 shows the relaxation test and the typical behavior to a steady strain. From the word viscoelastic it can be conducted that a viscoelastic material has both elastic behavior and viscous behavior. ordinary linear mechanical components like linear springs and linear dashpots can be used to construct a mechanical analogue of the constitutive models.

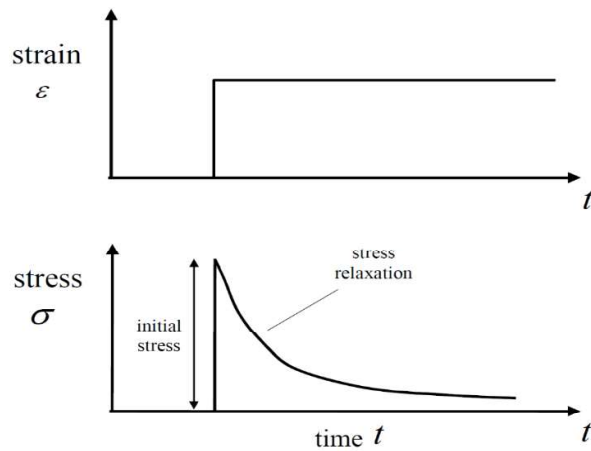


Figure 2.2. Relaxation test on a linear viscoelastic material (Lakes, 1998).

2.3.1. The Linear Elastic Solid (The Linear Spring)

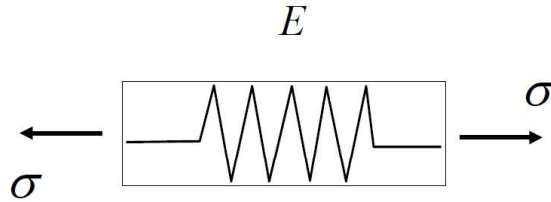


Figure 2.3. A linear spring (Lakes, 1998).

The easiest method to generate a material model is to presume that it is a linear spring of stiffness E which Hooke's law is the constitutive equation it (equation 2.4). It should be noticed that the spring responds immediately to the load and responds immediately to the load removal. The response can also be written as below:

$$\varepsilon = \sigma_o J \quad (2.14)$$

where J is the inverse of the stiffness which is called compliance.

2.3.2. The Linear Viscous Fluid (The Linear Dashpot)

The flow of Newtonian fluid limited by a moveable disk on top of it and a fixed disk in the bottom of it can be derived by the shear stress which is applied to the upper disk (figure 2.3). The fluid which is in touch with the upper disk moves fast since it has inhaled to it, but it cannot push the fluid which is in touch with the lower fixed disk. Thus a velocity gradient will be defined which is associated with the shear applied by the fluid's viscosity (η).

$$\frac{dv}{dy} = \frac{1}{\eta} \tau \quad (2.15)$$

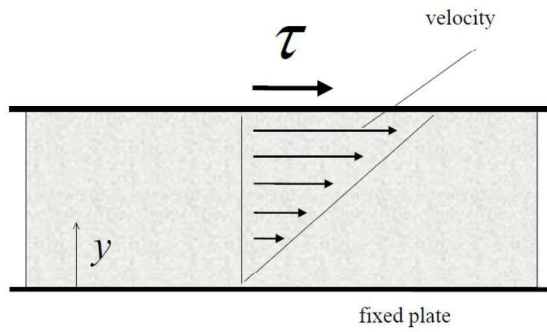


Figure 2.4. An ideal incompressible viscous fluid limited by a movable upper disk and a fixed lower disk (Lakes, 1998).

$$v = \frac{du_x}{dt} \quad (2.16)$$

The shear strain is:

$$\gamma = \frac{du_x}{dy} \quad (2.17)$$

Using equations 2.15 and 2.16:

$$\frac{dv}{dy} = \frac{d\gamma}{dt} \quad (2.18)$$

therefore,

$$\dot{\gamma} = \frac{1}{\eta} \tau \quad (2.19)$$

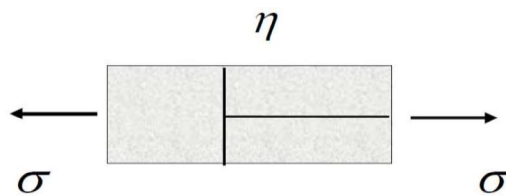


Figure 2.5. A linear dashpot (Lakes, 1998).

This concept of viscous fluid flow is utilized in the evaluation of viscoelastic materials, on the other hand, a dashpot (a piston moving in a viscous fluid with a viscosity of η) may constitute a viscous element (Lakes, 1998; Bland, 2016; Christensen, 2012).

$$\dot{\epsilon} = \frac{1}{\eta} \tau \tag{2.20}$$

Viscoelastic materials have some common characteristics, for instance, if they are stretched and then unloaded in a way they return to their original length the stress-strain relationships become different for loading and unloading called hysteresis. On the other hand, the mechanical energy required to deform the material cannot be recovered. By combining these two elements (springs and dashpots) in different ways, various classical models of viscoelastic material can be created (some of which are presented in figure 2.6).

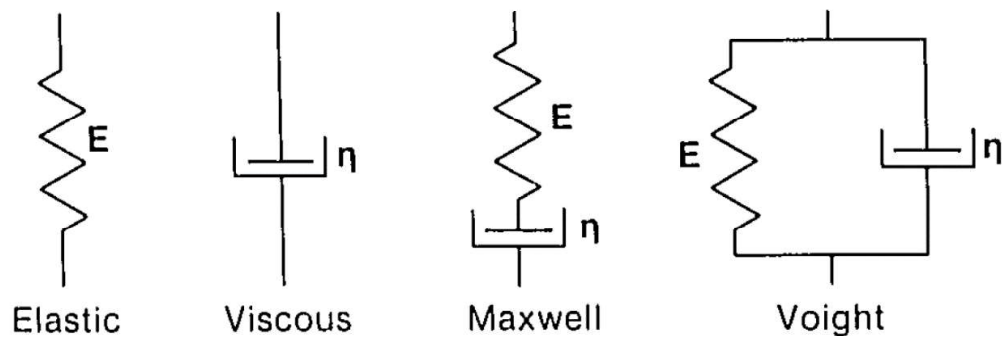


Figure 2.6. Classical viscoelastic material models. (Larrabee and Wayne, 1986).

2.4. Introduction to Fractional Calculus

Fractional Calculus is one of the mathematics' fields which came from the traditional definitions of the integral and derivative operators of calculus which in their non-integer exponents is a result of exponents with an integer value. The story of the appearance of fractional calculus backs to the year 1695 when L'Hospital asked Leibniz about a particular notation in his publication related to the derivative of a linear function $f(x) = \frac{d^n x}{dx^n}$. He asked what will happen if n be a non-integer number like 0.5. Leibniz answered: "An apparent paradox, from which one-day useful consequences will be drawn". There are many definitions in the topic of fractional calculus where the most famous ones are the Riemann-Liouville and Grünwald-Letnikov definitions. The last century was the turning point of the capability of fractional calculus in the engineering. Understanding of delimitation and utilizing fractional calculus will be made clearer by reviewing some mathematical definitions. These are the gamma function, the Laplace transform, and the Mittag-Leffler function which will be discussed in the following sections (Podlubny, 1999; Loverro, 2004).

2.4.1. The Gamma Function

Gamma function is one the most common function which is used in the fractional calculus. Its definition is:

$$\Gamma(x) = \int_0^{\infty} e^{-u} u^{x-1} du, \quad x \in \mathbb{R} \quad (2.21)$$

There are some noble properties related to gamma function:

$$\Gamma(x + 1) = x\Gamma(x) \quad (2.22)$$

$$\Gamma(x) = (x - 1)!, \quad \text{for } x \in \mathbb{N} \quad (2.23)$$

2.4.2. Laplace Transform and Convolution

The Laplace transform is a function transformation to solve complicated differential equations. The standard definition of it is as below:

$$L\{f(t)\} = \int_0^{\infty} e^{-st} f(t) dt = F(s) \quad (2.24)$$

One of the important usage of Laplace transform is the Laplace convolution:

$$f(t) * g(t) = \int_0^t f(t - \tau)g(\tau) d\tau = g(t) * f(t) \quad (2.9)$$

Sometimes the convolution of two functions cannot be solved easily in the domain of t but, in the domain of Laplace (s), the convolution comes up in the simpler product of functions:

$$L\{f(t) * g(t)\} = F(s)G(s) \quad (2.10)$$

2.4.3. The Mittag-Leffler Function

The Mittag-Leffler function is one the most important functions that has been utilized widely in this area. The Mittag-Leffler function plays the role of exponential function in the solution of non-integer order differential. The formal definition for this function is:

$$E_{\alpha,\beta}(x) = \sum_{k=0}^{\infty} \frac{x^k}{\Gamma(\alpha + \beta k)}, \alpha \in \mathbb{R} \quad \beta \in \mathbb{R}^+ \quad x \in \mathbb{C} \quad (2.11)$$

which is the two parameter Mittag-Leffler function, if $\alpha = 1$ then it will turn into one parameter Mittag-Leffler function.

If both parameters are equal to one, then the Mittag-Leffler function boils down to the exponential function:

$$E_{1,1}(x) = \exp(x) = e^x \quad (2.28)$$

The other important topic which should be mentioned about this function is the integration of it:

$$\frac{1}{\Gamma(\mu)} = \int_0^x (x-t)^{\mu-1} E_{\alpha,\beta}(\lambda t^\alpha) t^{\beta-1} dt = x^{\beta+\mu-1} E_{\alpha,\beta+\mu}(\lambda x^\alpha) \quad (2.29)$$

2.4.4. Grünwald-Letnikov and Riemann-Liouville Fractional Operators

The Grünwald–Letnikov derivative is a development of the derivative to derivate a function a non-integer number of times. It has been proposed by Anton Karl Grünwald and Aleksey Vasilievich Letkinov in 1868.

The first-order derivative of a continuous function like $g(t)$ is:

$$\dot{g}(t) = \frac{dg}{dt} = \lim_{h \rightarrow 0} \frac{g(t) - g(t-h)}{h} \quad (2.30)$$

The second order derivative of the same function can be written as:

$$\begin{aligned} \ddot{g}(t) &= \frac{d^2g}{dt^2} = \lim_{h \rightarrow 0} \frac{\dot{g}(t) - \dot{g}(t-h)}{h} \\ &= \lim_{h \rightarrow 0} \frac{g(t) - 2g(t-h) + g(t-2h)}{h^2} \end{aligned} \quad (2.31)$$

So if the function g be derivated m times:

$$g^{(m)}(t) = \frac{d^m g}{dt^m} = \lim_{h \rightarrow 0} \frac{1}{h^m} \sum_{n=0}^m (-1)^n \binom{m}{n} g(t-nh) \quad (2.32)$$

$$\binom{m}{n} = \frac{m(m-1)(m-2) \dots (m-n+1)}{n!} \quad (2.33)$$

then by replacing m with x ,

$$g_h^{(x)}(t) = \frac{1}{h^x} \sum_{n=0}^x (-1)^n \binom{x}{n} g(t-nh), \quad (2.34)$$

For negative values of m :

$$g_h^{(-x)}(t) = \frac{1}{h^x} \sum_{n=0}^x \binom{x}{n} g(t - nh), \quad (2.35)$$

where,

$$\binom{x}{n} = \frac{x(x+1)(x-2) \dots (x+n-1)}{n!} \quad (2.36)$$

$$\binom{-x}{n} = \frac{-x(-x-1)(-x-2) \dots (-x-n+1)}{n!} = (-1)^n \binom{x}{n} \quad (2.37)$$

then,

$$\lim_{h \rightarrow 0} g_h^{(-x)}(t) = {}_a D_t^{-x} g(t) \quad (2.38)$$

where ${}_a D_t^{-x} g(t)$ indicates a certain operation performed on the function $g(t)$, and a and t are the intervals related to the operator.

At the end it comes up with the following equation:

$${}_a D_t^{-x} g(t) = \lim_{h \rightarrow 0} h^x \sum_{n=0}^x \binom{x}{n} g(t - nh) = \frac{1}{(x-1)!} \int_a^t (t-\tau)^{x-1} g(\tau) d\tau \quad (2.39)$$

This equation represents the fractional derivative which is equivalent to the Riemann-Liouville fractional definition.

For positive values of m the fractional integration will be obtained:

$$\begin{aligned} {}_a D_t^x g(t) &= \lim_{h \rightarrow 0} h^{-x} \sum_{n=0}^x (-1)^n \binom{x}{n} g(t - nh) \\ &= \frac{1}{\Gamma(-x)} \int_a^t (t-\tau)^{-x-1} g(\tau) d\tau \end{aligned} \quad (2.40)$$

2.4.5. Caputo Fractional Operator

In the procedure of progress of fractional calculus, Riemann-Liouville definition had a noticeable role. In some special areas like the theory of viscoelasticity and hereditary solid mechanics, the concept of fractional derivative is very useful in terms of material properties characterization. The Riemann-Liouville method is an initial value approach. The initial value problems can be mathematically solved easily. However, since in the solutions of non-integer differential equations there is no known physical interpretation, their solutions are not studied widely. To tackle this problem, M. Caputo proposed Caputo's definition (Podlubny, 1999). It can be written as:

$${}_a^c D_t^\varphi g(t) = \frac{1}{\Gamma(\varphi - m)} \int_a^t \frac{g^{(m)}(\tau) d\tau}{(t - \tau)^{\varphi+1-m}} \quad (m - 1 < \varphi < m) \quad (2.41)$$

2.5. Fractional Calculus in the Theory of Viscoelasticity

In 1921 Nutting was the first person who introduced the topic of application of fractional calculus in the theory of viscoelasticity. He explained that the phenomenon of stress relaxation can be characterized by non-integer powers of time that contradict the strategy that stress relaxation is best characterized by decaying exponentials. In 1944 Scott-Blair utilized the theory of fractional calculus to model Nutting's early perceptions. Scott-Blair asserted the significance of studying the rheological characteristics of materials like rubber and plastics since they vary significantly from Newtonian or Hookean behavior in the rheological context. The equation below could describe the elasticity of an intermediate material that is neither real fluid nor perfectly elastic solid (Scott-Blair and Coppen, 1939):

$$S = \psi \sigma t^{-k} \quad (2.42)$$

where ψ determines elasticity and k is zero for an elastic solid and one for a Newtonian fluid.

In fact, Scott-Blair acquired a differential expression of non-integer order for these "intermediate" materials as follow:

$$\mathcal{X} = S / \frac{\partial^m \sigma}{\partial t^m} \quad (2.43)$$

He claimed that, in terms of gamma function, these kinds of functions can be solved; however, until that year, no one has tried to solve these equations.

In 1936 Gemant showed that fractional-order time derivatives can be utilized to model the viscoelastic conduct. Gemant was the first who suggested a non-integer order viscoelastic model which, a semi-derivative has substituted the first-order normal stress derivative of "Maxwell fluid model." To elucidate the definite distinction between the experimental outcomes acquired from viscoelastic samples and the Maxwell equation which is theoretical the Maxwell equation of viscoelastic bodies was semi-differentiated.

$$S = \frac{F}{\eta} + \frac{1}{(\eta E)^{1/2}} + \frac{d^{1/2} F}{dt^{1/2}} \quad (2.44)$$

In the equation above S , F , η and E represent the strain, the stress, the viscosity and the shear modulus of elasticity respectively.

In 1948 Gerasimov used derivatives of explicit fractional-order written as derivatives of Caputo to describe his viscoelastic model. Rabotnov chose to use Volterra integral operators in the same year with weakly unique kernels which have been explicated as non-integer integrals and derivatives. Moreover, Rabotnov claims that it is better to not mention the heredity phenomenon as a combination of Hookean elasticity and Newtonian viscosity, but as a main component of itself. The author therefore denies the rheology model depictions and stresses that the term "inherited elasticity" instead of word "viscoelasticity." To complete the meaning of "fading memory principle" he defined fractional exponential operators as Abel operator (I_α^*).

$$I_\alpha = \frac{t^\alpha}{\Gamma(1 + \alpha)} \quad (2.45)$$

In 1984, Koeller extended some of Rabotnov's viewpoint ideas and showed the relationship between fractional calculus and linear viscoelasticity theory. It has been demonstrated that Rabotnov's opinion which is related to hereditary solid mechanics is the same as having that the stress is proportional to the non-integer derivative of strain in damper. The notation of Rabotnov is generally utilized and the fractional calculus is relevant to the integral equation of Abel's theory (equation 2.46).

$$D^{-\varphi} f(t) = I_{\varphi}^* f(t) \quad (2.46)$$

and,

$$D^{\varphi} I_{\varphi}^* f(t) = f(t) \quad (2.47)$$

Based on what has been discussed one of the differences of non-integer derivatives with integer derivatives is heredity dependency of non-integer order derivatives. Ordinary derivatives are point functionals but since non-integer order derivatives possess the whole memory of past and since they are hereditary functionals, therefore, they are preferred to define the memory and hereditary properties of viscoelastic materials (Adolfsson et al., 2005). One of the privileges of this method is obtaining constitutive equations of viscoelastic materials with only few constants which have been determined from experiments (Soczkiewicz, 2002). To obtain the desired viscoelastic response observed through experiments, the phenomenological material models are developed by connecting mechanical elements such as springs and dashpots in various ways. Non-integer order viscoelastic models have an intermediate element between a linear elastic spring and a viscous dashpot termed as the spring-pot.

The dashpot in the classical Maxwell and Kelvin-Voigt components will be replaced by the spring-pot. For the fractional Maxwell, Kelvin-Voigt and three-element models, the creep and relaxation functions are derived using the theory of Hereditary Solid Mechanics which has been proposed by Rabotnov. Creep and relaxation functions are obtained in terms of the Mittag-Leffler function depending on the non-integer coefficient (φ). Also it has been shown that the non-integer order constitutive

law is a evolution from elastic solid conduct to Newtonian viscous fluid conduct when the "fractional coefficient" differs from zero to one. Unless the fractional coefficient is equivalent to unity, it has been indicated that there is no physical significance in the creep and relaxation times.

For linear models with homogeneity the Boltzmann superposition integral is available:

$$\sigma(t) = \int_{-\infty}^t R(t - \tau) \frac{d\varepsilon(\tau)}{d\tau} d\tau \quad (2.12)$$

In this equation R is the relaxation function.

$$R = \frac{E}{\Gamma(1 - \varphi)} \left(\frac{t}{\tau}\right)^{-\varphi} \quad (2.49)$$

By inserting equation 2.49 into equation 2.48:

$$\sigma(t) = \frac{E\tau^\varphi}{\Gamma(1 - \varphi)} \int_{-\infty}^t (t - \tau)^{-\varphi} \frac{d\varepsilon(\tau)}{d\tau} d\tau \quad (2.50)$$

The equation 2.50 composed of two intervals, the first interval is from $-\infty$ to zero, and the other interval is from zero to t. To solve this equation, the Riemann expression can be utilized as follows:

$${}_a D_t^\varphi g(t) = \frac{1}{\Gamma(\varphi)} \int_a^t g(\tau) (t - \tau)^{\varphi-1} d\tau \quad (2.51)$$

For $\varphi > 0$ if $a = 0$ then the equation turns into Riemann-Liouville formulation and if $a = -\infty$, it becomes the Weyl's formula.

$$\sigma(t) = E\tau^\varphi \frac{d^{\varphi-1}}{dt^{\varphi-1}} \frac{d\varepsilon(t)}{dt} = E\tau^\varphi \frac{d^\varphi \varepsilon(t)}{dt^\varphi} \quad (2.52)$$

The models in figure 2.6 are composed of a small number of single elements (Ward, 1983; Tschoegl, 1989). The difficulty is the limited sort of solutions which causes the inadequate quantification for the model. To tackle this problem, the stress and strain could be related using fractional equations. Using fractional calculus by varying φ in equation 2.52 from zero to one, an intermediate behavior between viscous and elastic conduct can be obtained. The equation 2.52 can be represented by hierarchical formations of springs and dashpots (figure 2.7). A fractional element to describe such a hierarchical formation was proposed (figure 2.8 (c)) which schematically simulate a ladder such as the one drawn in figure 2.7 (Schiessel et al., 1995).

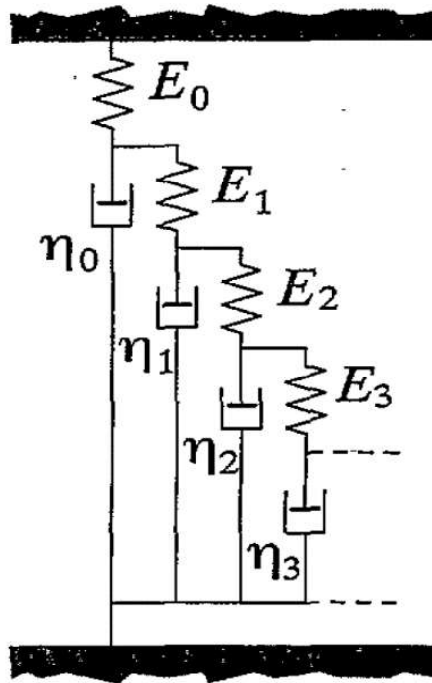


Figure 2.7. Sequential realization of the frictional element (Schiessel et al., 1995).

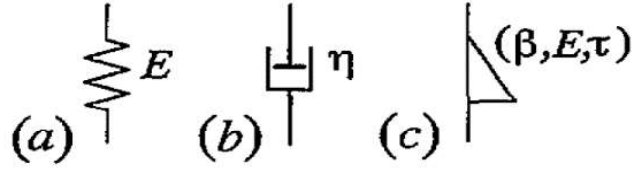


Figure 2.8. (a) elastic, (b) viscous and (c) fractional element (Schiessel et al., 1995).

The constitutive equation for a fractional element is:

$$\sigma(t) = E\eta^\varphi \frac{d^\varphi \varepsilon}{dt^\varphi}, \quad 0 \leq \varphi \leq 1 \quad (2.53)$$

φ is the non-dimensional fractional coefficient.

To be evident if φ be equal to zero the material has perfect memory and shows a solid case and when φ is equal to one the material has no memory describing a fluid case. Fractional coefficient φ is the power-law response found on most viscoelastic materials. The relaxation function does not generally follow a straightforward exponential but is defined by an expression of power law (equation 2.54).

$$R(t) = \frac{E}{\Gamma(1 - \varphi)} \left(\frac{t}{\tau}\right)^\varphi \quad (2.54)$$

where τ is the time constant.

The creep compliance for a fractional element will be:

$$C(t) = \frac{1}{E\Gamma(1 + \varphi)} \left(\frac{t}{\tau}\right)^{-\varphi} \quad (2.55)$$

As mentioned before the dashpot in the classical viscoelastic models is replaced by the "spring-pot" for the linear non-integer order viscoelastic models. By changing the value of the fractional coefficient, an extensive domain of responses could be obtained using a spring-pot in classical linear viscoelastic models.

Equations 2.54 and 2.55 can be derived by taking the following steps (Schiessel et al., 1995):

Here is the definition of Fourier transform:

$$F\{g(t); \omega\} = \tilde{g}(\omega) = \int_{-\infty}^{+\infty} g(t)e^{-i\omega t} dt \quad (2.56)$$

Since,

$$F\left\{\frac{d^\varphi g(t)}{dt^\varphi}; \omega\right\} = (i\omega)^\varphi \tilde{g}(\omega) \quad (2.57)$$

Then Fourier transform of equation 2.52 will be:

$$\tilde{\sigma}(\omega) = E(i\omega\tau)^\varphi \tilde{\varepsilon}(\omega) \quad (2.58)$$

The complex modulus is:

$$R^*(\omega) = \frac{\tilde{\sigma}(\omega)}{\tilde{\varepsilon}(\omega)} \quad (2.59)$$

then,

$$R^*(\omega) = E(i\omega\tau)^\varphi \quad (2.60)$$

In order to derive the relaxation modulus R two different ways can be taken:

- Using the storage modulus: $R'(\omega) = Re(R^*(\omega))$

$$R(t) = \frac{2}{\pi} \int_0^\infty \frac{R'(\omega)}{\omega} \sin(\omega t) d\omega = F_s^{-1} \left\{ \frac{R'(\omega)}{\omega}; t \right\} \quad (2.61)$$

- Using the loss modulus: $R''(\omega) = Im(R^*(\omega))$

$$R(t) = \frac{2}{\pi} \int_0^\infty \frac{R''(\omega)}{\omega} \cos(\omega t) d\omega = F_s^{-1} \left\{ \frac{R''(\omega)}{\omega}; t \right\} \quad (2.62)$$

For a single fractional element, the relaxation modulus obtained as:

$$R(t) = F_s^{-1} \left\{ E \tau^\varphi \cos \left(\frac{\pi\varphi}{2} \omega^{\varphi-1} \right); t \right\} = \frac{E}{\Gamma(1-\varphi)} \left(\frac{t}{\tau} \right)^{-\varphi} \quad (2.63)$$

For the creep compliance:

$$C^*(\omega) = \frac{1}{R^*(\omega)} \quad (2.64)$$

then,

$$C(t) = \frac{1}{E\Gamma(1+\varphi)} \left(\frac{t}{\tau} \right)^\varphi \quad (2.65)$$

2.6. The Quasi-Linear Viscoelastic Theory (QLV)

Linear theory of viscoelasticity refers well to viscoelastic materials for infinitesimal strain. However, the non-linear stress-strain properties and viscoelastic response which is dependent on time and history are given by theory proposed by Fung in 1993 called the quasi-linear viscoelastic (QLV) method which is provided for finite strain problems. In this theorem, the multiplication of a reduced relaxation function and a non-linear elastic response is specified as the relaxation function, where the reduced relaxation function and the elastic response are functions of time and strain only respectively. Therefore, there is a separable non-linear viscoelasticity kernel and the stress function is developed owing to the strain applied by using the superposition principle. The separable stress function is characterized by a reduced relaxation function ($R(t)$) and an instant elastic response ($\sigma^{(e)}(\varepsilon)$).

$$\sigma(\varepsilon(t), t) = R(t) * \sigma^{(e)}(\varepsilon) \quad (2.66)$$

Using the superposition principle for $t > \tau$,

$$\sigma(\varepsilon(t), t) = \int_{-\infty}^t R(t-\tau) \frac{\partial \sigma^{(e)}(\varepsilon(t-\tau))}{\partial \varepsilon} \frac{\partial \varepsilon}{\partial \tau} d\tau \quad (2.67)$$

Therefore, at the time t the stress is a summation of all past changes contributions. This equation is a "hereditary integral," and stress at each moment is dependent on everything that has occurred in the past, on the whole history of stress. The lower limit of the integral supposed as which implies that the integration takes place before the motion starts. By replacing zero for the lower limit of integral the experimental condition can be represented. QLV model utilizes a continuous spectrum reduced relaxation function, which implies an unlimited number of series-lined standard linear solid models (figure 2.9).

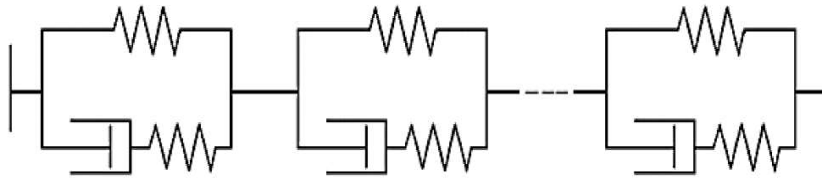


Figure 2.9. Unlimited number of series-connected standard linear solid models (Fung, 1993).

For this model Fung proposed a reduced relaxation function as below:

$$R(t) = \frac{1 + c \left(E \left(\frac{t}{\tau_2} \right) - E \left(\frac{t}{\tau_1} \right) \right)}{1 + c \ln \left(\frac{\tau_2}{\tau_1} \right)} \quad (2.68)$$

where, $E(\cdot)$ is the first exponential integral, c is the viscoelasticity degree of the material called the dimensionless positive constant, τ_1 and τ_2 are the short term and long term viscoelastic time constants respectively. In 2008 Craiem et al. stated that estimating the material constants of this reduced relaxation function because of the relatively larger number of parameters is problematic also it shows low sensitivity during procedures of adaptation.

2.7. The Fractional Order Viscoelastic Model (FOV)

In 2005 Doehring et al. proposed a way to use a fractional order viscoelastic (FOV) model instead of QLV in modeling the material properties. FOV model uses a fractional order integral to explain the material behavior. As presented in figure 2.9 as well a description of the QLV model is an infinite series of standard linear solid models connected in series. If the all responses of those elements will be summated a wide and flat frequency response can be obtained, but the FOV model obeys a hierarchical structure to generate the connectivity between elements, which leads to a fractal type tree model (figure 2.10). There is an order of evolution, which is the non-integer order of integration (φ), which determines the depth and branching of the tree. If φ equals to 1, the model acts like a Newtonian fluid and when it is zero, the response will be purely elastic. Doehring et al. implemented QLV and its equivalent FOV constitutive models in 1-D to extract their material constants for aortic valve cusp tissue. They compared the results of both methods and the model with FOV constitutive law even was more accurate than the one with QLV. The other advantage of using the fractional method was extracting lower numbers of material parameters than QLV. In the FOV's formulation just like QLV the concept of separating the material response into non-linear elastic and linear viscoelastic behavior has been used. The only difference was using a function which includes the Mittag-Leffler function instead of using the relaxation function (equation 2.27).

$$R(t) = \left(\frac{\tau}{\rho}\right)^\varphi + \left(1 - \left(\frac{\tau}{\rho}\right)^\varphi\right) E_{\varphi,1} \left(-\left(\frac{t}{\tau}\right)^\varphi\right) \quad (2.69)$$

where τ and ρ are the short-term relaxation time constant and the long-term creep time constant respectively.

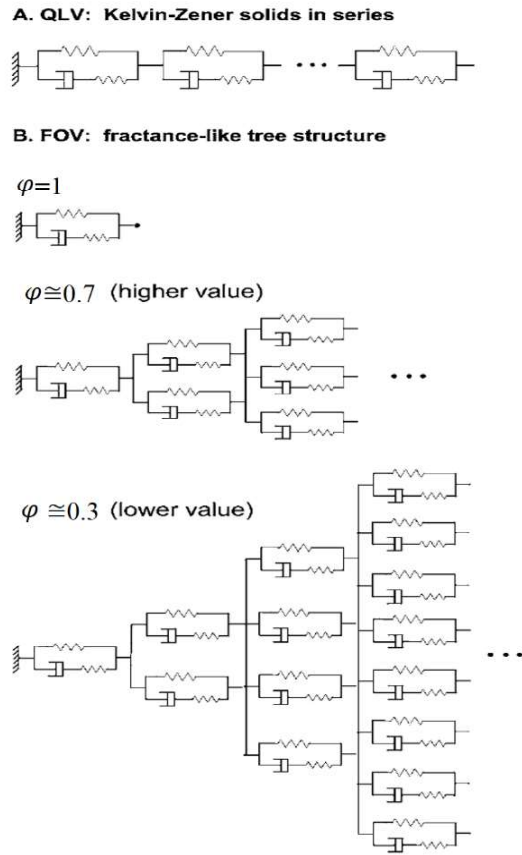


Figure 2.10. QLV (serial) and FOV (fractional) model spring and dashpot representations. (a) FOV may be depicted with a fractal tree model (b) varying in width and depth based on the fractional order φ (Doehring et al., 2005).

In 2005 Freed et al. had an investigation on choosing the best mechanical model between four elastic functions and five viscoelastic kernel functions using the compression and stress relaxation tests of Miller–Young et al. (2002) to model the human calcaneal fat pad. They used the K-BKZ theory (Kaye, 1962; Bernstein et al., 1963) which utilizes the strain energy function for providing the tensor form of the viscoelastic model. The best viscoelastic model has been chosen between generalized Maxwell model, the stretched exponential Kohlrausch-William-Watts, the QLV model, the FOV model, and a regularized fractional-derivative model. At the end using

The Akaike information criterion (AIC) information theoretic (Burnham and Anderson, 2002) a power law and a regularized fractional derivative is shown to have the best response for the elastic part and the viscoelastic kernel respectively.

2.8. Implementing Viscoelastic Models Using Strain Energy Density Function

Strain energy is the work to be accomplished in the reference state on the unit volume of the body to deform it to the current configuration (Fung, 1993). In 1975 James et al. proposed two analytical formulations for the strain energy function for isotropic and incompressible bodies having five or nine material parameters. The method of changing or modifying a strain energy function in accordance with a data set is a "three-dimensional analogue of simple curve-fitting" (Treloar, 1949). For instance, for materials which are isotropic, the strain energy function should be a function of both left and right Cauchy deformation tensors strain invariants. Known instances are models of materials such as Mooney in 1940, Rivlin in 1947 and Rivlin in 1965. If a material be perfectly elastic, there is a strain energy function W , determined per unit volume of the body in the current configuration and the body is termed as "hyperelastic" or "Green elastic" when the material has a strain-energy function, which is in terms of a scalar function of one of the strains and deformation tensors whose derivative determines the stress component with respect to the strain component (equation 2.70) (Malvern, 1969).

$$S_{ij} = \frac{\partial W(E)}{\partial E_{ij}} = 2 \frac{\partial W(C)}{\partial C_{ij}}, \quad i, j = 1, 2, 3 \quad (2.70)$$

where, $W(E)$, E , C and S are the strain energy per unit volume for the current configuration, the Green-Lagrange finite strain tensor, the symmetric right Cauchy-Green deformation tensor and the symmetric second Piola-Kirchoff stress tensor respectively.

For isotropic materials when they are deformed the elastic strain energy W could be defined as a function of the strain invariants of Green-Lagrange finite strain tensors I_1 , I_2 and I_3 (James et al., 1975).

$$W = \sum_{i,j,k=0}^{\infty} C_{ijk} (I_1 - 3)^i (I_2 - 3)^j (I_3 - 3)^k \quad (2.71)$$

$$I_1 = \lambda_1^2 + \lambda_2^2 + \lambda_3^2 \quad (2.72)$$

$$I_2 = \lambda_1^2 \lambda_2^2 + \lambda_2^2 \lambda_3^2 + \lambda_1^2 \lambda_3^2 \quad (2.73)$$

$$I_3 = \lambda_1^2 \lambda_2^2 \lambda_3^2 \quad (2.74)$$

where, C_{ijk} are the material parameter constants and λ is the principal stretch.

For incompressible materials ($\lambda_1 \lambda_2 \lambda_3 = 1$ and $I_3 = 1$) the strain energy density function becomes as below:

$$W = \sum_{i,j=0}^{\infty} C_{ij} (I_1 - 3)^i (I_2 - 3)^j \quad (2.75)$$

The temperature is supposed to remain constant throughout these formulations, (isothermal mechanical behavior) and the strain energy function is dependent only on the end-state strain and not on the strain history (Ogden R. W., 1972). Incompressible materials have high effective bulk modulus, therefore, the big volumetric stresses are as a result of small volumetric strains, the hydrostatic part of the stress tensor is so sensitive to the variations in the hydrostatic strain. To tackle this difficulty, the strain energy function has been divided into deviatoric and volumetric parts (Malkus and Hughes, 1978; Liu and Choudhry, 2004). As regards volumetric and deviatoric deformations, the elastic and inelastic characteristics of a certain material often display distinct behaviors. This needs the additive splitting of the strain energy function as a function of principal strain invariants (equation 2.76) and principal stretch ratios (equation 2.77).

$$\psi = U(J) + W(\bar{I}_1, \bar{I}_2) \quad (2.76)$$

$$\psi = U(J) + W(\bar{\lambda}_1, \bar{\lambda}_2, \bar{\lambda}_3) \quad (2.77)$$

U is the deviatoric part of the strain energy function which has been defined in terms of the tensor ($J = \det (F)$). For incompressible materials Jacobian is equal to one. A time-dependent strain energy function could be described as a product of an elastic strain energy function which is non-linear and a stress relaxation function which is time-dependent (when stress is acquired from strain) or a creep compliance which is time-dependent (when strain is derived from stress).

Although many Mooney material formulations are utilized in literature to model the in-vivo indentation of bulk muscular soft tissue. In 2004 Tonuk and Silver-Thorn used the extended form of viscoelastic the James-Green-Simpson nonlinear elastic material formulation which is the third-order deformation Mooney, to simulate the time-dependent mechanical behavior of residual limb soft tissues to indentation. They simulated their model using a generalized linear Kelvin-Voigt material model (figure 2.11).

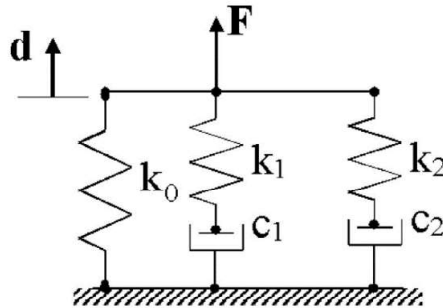


Figure 2.11. A generalized linear Kelvin-Voigt material model (Tonuk and Silver-Thorn, 2004).

Equation 2.73 is a strain energy density function in relaxation form. W_0 is the instant strain energy density and the term in the bracket is the two terms Prony series representation which represents the constitutive law of the generalized Kelvin-Voigt linear viscoelastic material model. δ_1 and δ_2 are the short and long-term relaxation magnitude and τ is the time constant.

$$W(t) = W_0 \left[1 - \delta_1 \left(1 - e^{-\frac{t}{\tau_1}} \right) - \delta_2 \left(1 - e^{-\frac{t}{\tau_2}} \right) \right] \quad (2.78)$$

It has been shown that the viscoelastic model of three-element fractional order standard linear solid model fits the experimental outcomes better than the representation. Therefore, a correction for the above formulation is proposed so that three-element fractional order relaxation function can be replaced by the two term Prony series. Therefore, equation 2.73 turns into equation 2.74. It can be concluded that the number of constants to be estimated are decreased by incorporating non-integer order derivatives in constitutive relationships since, the total number of constants becomes nine for this formulation (5 nonlinear elastic constants and 4 viscoelastic constants for three elements), which is fewer than the number of constants used in the ten-parameter two-term Prony series representation (five nonlinear elastic parameters and five viscoelastic constants for each element) (Demirci and Tonuk, 2014).

$$W(t) = W_0 \left[1 - \frac{\frac{E_1}{E_2}}{1 + \frac{E_1}{E_2}} \left\{ 1 - E_\varphi \left(- \left(\frac{t}{\tau} \right)^\varphi \right) \right\} \right] \quad (2.79)$$

$$W_0 = C_{10}(I_1 - 3) + C_{01}(I_2 - 3) + C_{11}(I_1 - 3)(I_2 - 3) + C_{20}(I_1 - 3)^2 + C_{30}(I_1 - 3)^3 \quad (2.80)$$

In 2014 Demirci and Tonuk developed a user subroutine which was written in FORTRAN for equation above which have been implemented to finite element software MSC. MARC Using first and second principal stretch ratios, the instantaneous (glassy) strain energy density function was defined. The bulk modulus of soft tissue was modeled as 1000 times the initial tangent modulus which turned out to be nearly incompressible material. The user subroutine and finite element model using this subroutine were exhaustively checked against known responses and the accuracy was found to be satisfactory.

In order to determine the capability of non-integer order material model for simulating soft biological tissues, in-vivo experiments have been done on human fore-arm bulk soft tissues. A computer controlled custom-made indenter having a step motor and a loadcell to measure tissue reaction force are utilized to perform these experiments (Petekkaya and Tonuk, 2011). The non-integer order relaxation and creep functions were tested against experimental force-relaxation and creep data. Cyclic loading and unloading, relaxation and creep experimental data was used in inverse finite element modeling with non-integer order viscoelastic material model for the purpose of material parameter identification.

The results showed that the optimization of material coefficients which have been gained using relaxation experiments with creep experimental data can simulate relaxation, creep and cyclic loading and unloading experiments. The non-integer order time dependent behavior was found to be a good candidate for simulating indentation experiment of the soft biological tissues. Structural or micro-structural elastic material models together with non-integer time dependent behavior may supply better insight to observed mechanical behavior of soft biological tissues however obtaining structural or micro-structural information of the soft tissue to be modelled might not be as simple as performing indentation experiments.

In 2008 Bummo and Jung extracted the material characterization of the porcine liver. For the experiment part, in-vitro indentation tests have been utilized using a hemisphere tip indenter and an electromechanical indentation system. In order to model the tissue behavior, they used the quasilinear viscoelastic framework (Fung, 1996). This hypothesis divides the mechanical behavior into a linear viscoelastic stress- relaxation response and a time-independent elastic response which for the elastic response a hyperelastic material model. By separating the material model into the models which were mentioned the procedure of estimating material parameters reduced considerably. The least squares method in MATLAB has been used in order to get the constants of the viscoelastic model, and then parameters related to the hyperelastic model were extracted using the inverse finite element approach.

Many methods have been proposed to derive non-integer derivative constitutive models. In 2015 Fukunaga and Shimizu proposed a method for finite deformation of viscoelastic bodies to generate the non-integer derivative constitutive equations. One of the potent ways in establishing 3D fractional constitutive laws is using the generalized Maxwell model (figure 2.12) for a viscoelastic material. Since the origin of dynamical conduct of the viscoelastic bodies is from different combinations of elastic and viscous elements, the strain energy of the elastic elements has an important role in deriving the non-integer derivative constitutive law. A generalization of an objective time rate of strain to non-integer order represents the non-integer derivative model. Then, the method can be used to determine a non-integer derivative model as a function of the second Piola–Kirchhoff stress. Also, another non-integer derivative model is obtained as a function of the Biot stress tensor. At the end, both of those methods have been compared to each other and the data fitted well.

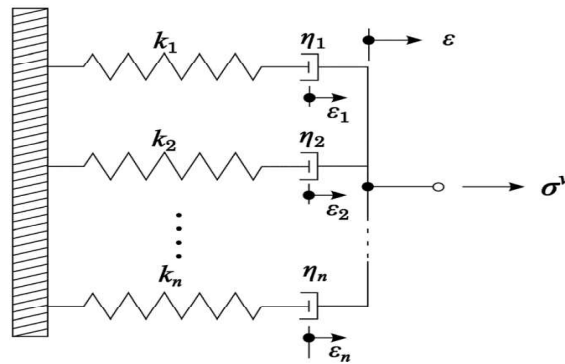


Figure 2.12. The Generalized Maxwell Model (Fukunaga and Shimizu, 2015).

2.9. Implementing Viscoelastic Models Using Boltzmann Superposition

Utilizing the strain energy function is not the only way to implement viscoelastic material models into finite element codes. Another method which can be used is using the matrix of Jacobian. To obtain the Jacobian of the viscoelastic model for each

instant of time from the constitutive equation the Boltzmann superposition principle (equation 2.48) is a good solution since it gives the strain history for any stress distribution when the creep function is available and gives the stress history when there is relaxation function (Alotta et al., 2018). Although convolution works for linear functions for this specific problem by taking small time increments Boltzmann superposition can be utilized.

$$\varepsilon(t) = \int_0^t C(t - \tau) \dot{\sigma}(\tau) d\tau \quad (2.81)$$

$$\sigma(t) = \int_0^t R(t - \tau) \dot{\varepsilon}(\tau) d\tau \quad (2.82)$$

where, the creep function is:

$$C(t) = \frac{t^\varphi}{B_\varphi \Gamma(1 + \varphi)} \quad (2.83)$$

And the relaxation function is:

$$R(t) = \frac{B_\varphi t^{-\varphi}}{\Gamma(1 - \varphi)} \quad (2.84)$$

Then by implementing creep and relaxation functions in equations above:

$$\varepsilon(t) = \frac{1}{B_\varphi \Gamma(1 + \varphi)} \int_0^t (t - \tau)^{\varphi-1} \sigma(\tau) d\tau = \frac{1}{B_\varphi} (I_{0+}^\varphi \sigma)(t) \quad (2.85)$$

$$\sigma(t) = \frac{B_\varphi}{\Gamma(1 - \varphi)} \int_0^t (t - \tau)^{-\varphi} \dot{\varepsilon}(\tau) d\tau = B_\varphi (D_{0+}^\varphi \varepsilon)(t) \quad (2.86)$$

$(I_{0+}^\varphi \sigma)(t)$ is the Riemann-Liouville fractional integral and $(D_{0+}^\varphi \varepsilon)(t)$ is the Caputo's non-integer derivative of order φ . Where φ is between zero and one and B_φ is its viscosity coefficient.

In this study, the fractional 3-D constitutive models are evaluated using the same approach (Boltzmann superposition principle) and their numerical solution to implement in the finite element software ABAQUS/Standard have been developed. In the next chapter, the method used in this survey is explained in detail.

CHAPTER 3

METHODOLOGY

3.1. Grünwald Coefficient

As mentioned in Chapter 2, the integer-order derivative of function $g(t)$ is:

$$\frac{d^m g(t)}{dt^m} = \lim_{\Delta t \rightarrow 0} [(\Delta t)^{-m} \sum_{n=0}^m (-1)^n \binom{m}{n} g(t - i\Delta t)], \quad (3.13)$$

where, for integer n and m and for $0 \leq n \leq m$:

$$\binom{m}{n} = \frac{m!}{n!(m-n)!} \quad (3.14)$$

and for $0 \leq m \leq n$:

$$\binom{m}{n} = 0 \quad (3.3)$$

By replacing $\frac{t}{P}$ instead of Δt equation 3.1 becomes:

$$\frac{d^m g(t)}{dt^m} = \lim_{P \rightarrow \infty} \left[\left(\frac{t}{P} \right)^{-m} \sum_{n=0}^{P-1} (-1)^n \binom{m}{n} g \left(t - n \frac{t}{P} \right) \right] \quad (3.4)$$

where, $P = 1, 2, 3, \dots$

To use the equation 3.4 for non-integer m and integer $n > 0$, $\binom{m}{n}$ can be replaced by (m has been replaced by r):

$$\binom{r}{n} = \frac{r(r-1)(r-2) \dots (r-n+1)}{n!} \quad (3.5)$$

for $n = 0$,

$$\binom{r}{n} = 1 \quad (3.6)$$

for $n \geq 0$,

$$(-1)^n \binom{r}{n} = \binom{n-r-1}{n} = \frac{\Gamma(n-r)}{\Gamma(-r)\Gamma(n+1)} \quad (3.7)$$

Then, the Grünwald fractional derivative for non-integer φ will be derived:

$$\frac{d^\varphi g(t)}{dt^\varphi} = \lim_{P \rightarrow \infty} \left[\left(\frac{t}{P}\right)^{-\varphi} \sum_{n=0}^{P-1} \frac{\Gamma(n-\varphi)}{\Gamma(-\varphi)\Gamma(n+1)} g\left(t - n\frac{t}{P}\right) \right] \quad (3.8)$$

where,

$$\mu_{n+1}^{(\varphi)} = \frac{\Gamma(n-\varphi)}{\Gamma(-\varphi)\Gamma(n+1)} \quad (3.9)$$

$\mu_{n+1}^{(\varphi)}$ is the Grünwald coefficient.

To be able to implement the fractional derivative into finite element software its numerical solution should be evaluated. Similar to the numerical integral assessment, non-integer derivatives could be calculated by approximating the infinite sum in Equation 3.8 by a finite sum, such that $P < \infty$, thus, $\frac{d^\varphi g(t)}{dt^\varphi}$ can be roughly assessed as follows:

$$\frac{d^\varphi g(t)}{dt^\varphi} \approx \left(\frac{t}{P}\right)^{-\varphi} \sum_{n=0}^{P-1} \mu_{n+1}^{(\varphi)} g\left(t - n\frac{t}{P}\right) \quad (3.15)$$

Using the property of fading memory which has been introduced by Podlubny in 1999, the numerical evaluation of Grünwald coefficient is equation 3.14 (Schmidt and Gaul,2002).

Since,

$$\Gamma(a) = (a - 1)\Gamma(a - 1) \quad (3.16)$$

Then,

$$\Gamma(n - \varphi) = (n - \varphi - 1)\Gamma(n - \varphi - 1) \quad (3.17)$$

$$\Gamma(n + 1) = n\Gamma(n) \quad (3.18)$$

$$\begin{aligned} \mu_{n+1}^{(\varphi)} &= \frac{\Gamma(n - \varphi)}{\Gamma(-\varphi)\Gamma(n + 1)} = \frac{(n - \varphi - 1)\Gamma(n - \varphi - 1)}{n\Gamma(-\varphi)\Gamma(n)} \\ &= \frac{(n - \varphi - 1)}{n} \mu_n^{(\varphi)} \end{aligned} \quad (3.19)$$

Based on creep and relaxation experiments which were done on different materials like polymers, rubbers, etc. It has been found that for the simplest case where only one stress component (hydrostatic or deviatoric stress) is available, their creep or relaxation behavior can be fitted by power laws of real order, so the creep and relaxation functions can be defined as below (Tovrik and Bagley, 1984; Nutting, 1921):

$$R(t) = \frac{B_\varphi t^{-\varphi}}{\Gamma(1 - \varphi)} \quad (3.20)$$

$$C(t) = \frac{t^\varphi}{B_\varphi \Gamma(1 + \varphi)} \quad (3.21)$$

where, B_φ is the material parameter which can be obtained by curve fitting.

As discussed in previous chapter in the domain of linear viscoelasticity the Boltzmann superposition principle is valid therefore:

when the relaxation function is available the stress in terms of strain history is:

$$\sigma(t) = \int_0^t R(t - \tau) \dot{\epsilon}(\tau) d\tau \quad (3.22)$$

and when the creep function is available the strain in terms of stress history is:

$$\varepsilon(t) = \int_0^t C(t - \tau) \dot{\sigma}(\tau) d\tau \quad (3.18)$$

Equations 3.17 and 3.18 are mostly called hereditary integrals.

3.2. Generalizing a 3-D Isotropic Constitutive Law for a FKV Model

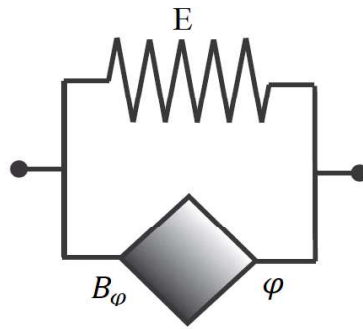


Figure 3.1. Fractional Kelvin-Voigt (FKV) model.

For a fractional Kelvin-Voigt model the relaxation and creep functions are as below:

$$R(t) = E + \frac{B_\varphi t^{-\varphi}}{\Gamma(1 - \varphi)} \quad (3.19)$$

$$C(t) = \frac{1}{E} - \frac{1}{E} E_\varphi \left(-\frac{E}{B_\varphi} t^\varphi \right) \quad (3.23)$$

where E_φ is the one parameter Mittag-Leffler function which can be evaluated using equation 2.11 by taking α as one.

Also, the relaxation and creep tensors for an isotropic material are as follows:

$$R_{ijkh}(t) = \left(K_R(t) - \frac{2}{3} G_R(t) \right) \delta_{ij} \delta_{kh} + G_R(t) (\delta_{ik} \delta_{jh} + \delta_{ih} \delta_{jk}) \quad (3.24)$$

$$C_{ijkh}(t) = \left(\frac{1}{9} K_C(t) - \frac{1}{6} G_C(t) \right) \delta_{ij} \delta_{kh} + G_C(t) \left(\delta_{ik} \delta_{jh} - \frac{1}{2} \delta_{ih} \delta_{jk} \right) \quad (3.25)$$

Where $K_R(t)$ and $G_R(t)$ are the volumetric and deviatoric relaxation functions and $K_C(t)$ and $G_C(t)$ are the volumetric and deviatoric creep functions respectively.

Here to generate the behavior of fractional Kelvin-Voigt model the relaxation function has been utilized.

The tensor form of the Boltzmann superposition principle is:

$$\sigma_{ij}(t) = \int_0^t R_{ijkh}(t - \tau) \dot{\epsilon}_{kh}(\tau) d\tau \quad (3.23)$$

By substituting equation 3.21 into Boltzmann superposition principle a constitutive law for the fractional Kelvin-Voigt model will be obtained.

$$\begin{aligned} \sigma_{ij}(t) = \int_0^t \left(K_R(t - \tau) - \frac{2}{3} G_R(t - \tau) \right) \dot{\epsilon}_{ij}(\tau) d\tau \\ + \int_0^t G_R(t - \tau) (\delta_{ik} \delta_{jh} + \delta_{ih} \delta_{jk}) \dot{\epsilon}_{kh}(\tau) d\tau \end{aligned} \quad (3.24)$$

$$K_R(t) = K + \frac{K_\theta t^{-\theta}}{\Gamma(1 - \theta)} \quad (3.25)$$

$$G_R(t) = G + \frac{G_\beta t^{-\beta}}{\Gamma(1 - \beta)} \quad (3.26)$$

Equations 3.27 and 3.28 are power law functions for the volumetric and deviatoric relaxation functions respectively which have been derived by means of equation 3.19. where K_θ and G_β are the anomalous bulk and shear relaxation moduli, respectively. β and θ are real numbers indicating the orders of bulk and shear power laws, respectively.

3.3. Numerical Evaluation of the Constitutive Model of FKV

In order to evaluate the numerical solution of the constitutive model (equation 3.24) there are two different equations for normal and shear stresses.

3.3.1. Normal Stresses

To obtain the constitutive equation for normal stresses, the procedure is as follows:

$i = j$, and also by considering $i = 1$,

$$\begin{aligned} \sigma_{11}(t) = \int_0^t \left(K_R(t - \tau) - \frac{2}{3} G_R(t - \tau) \right) \dot{\epsilon}_s(\tau) d\tau \\ + 2 \int_0^t G_C(t - \tau) \dot{\epsilon}_{11}(\tau) d\tau \end{aligned} \quad (3.27)$$

where,

$$\dot{\epsilon}_s = (\dot{\epsilon}_{11} + \dot{\epsilon}_{33} + \dot{\epsilon}_{33}) \quad (3.28)$$

By considering deviatoric and volumetric relaxation functions as equation 3.25 and equation 3.26 the constitutive equation for the $k + 1^{st}$ time increment is:

$$\begin{aligned}
\sigma_{11,k+1} &= K\varepsilon_{s,k+1} + 2G\varepsilon_{11,k+1} - \frac{2}{3}G\varepsilon_{s,k+1} \\
&\quad + \frac{K_\theta}{\Gamma(1-\theta)} \int_0^t (t-\tau)^{-\theta} \dot{\varepsilon}_{s,k+1} d\tau \\
&\quad - \frac{2}{3} \frac{G_\beta}{\Gamma(1-\beta)} \int_0^t (t-\tau)^{-\beta} \dot{\varepsilon}_{s,k+1} d\tau \\
&\quad + 2 \frac{G_\beta}{\Gamma(1-\beta)} \int_0^t (t-\tau)^{-\beta} \dot{\varepsilon}_{11,k+1} d\tau
\end{aligned} \tag{3.29}$$

Using what Podlubny has proved for fractional derivatives in his text book the integrals in the equation 3.29 can be solved as:

$$\frac{K_\theta}{\Gamma(1-\theta)} \int_0^t (t-\tau)^{-\theta} \dot{\varepsilon}(\tau) d\tau = K_\theta ({}_0^C D_t^\theta \varepsilon) \tag{3.30}$$

Equation 3.30 is the Caputo fractional derivative of order φ .

Equation 3.10 (${}_0^C \bar{D}_t^\theta \varepsilon$) will be evaluated numerically using equation 3.14 and the constitutive equation turns into the following equation:

$$\begin{aligned}
\sigma_{11,k+1} &= K\varepsilon_{s,k+1} + 2G\varepsilon_{11,k+1} - \frac{2}{3}G\varepsilon_{s,k+1} + K_\theta \Delta t^{-\theta} \sum_{n=1}^{k+1} \mu_n^{(\theta)} \varepsilon_{s,k-n+2} \\
&\quad - \frac{2}{3} G_\beta \Delta t^{-\beta} \sum_{n=1}^{n+1} \mu_n^{(\beta)} \varepsilon_{s,k-n+2} \\
&\quad + 2G_\beta \Delta t^{-\beta} \sum_{n=1}^{k+1} \mu_n^{(\beta)} \varepsilon_{11,k-n+2}
\end{aligned} \tag{3.31}$$

$\sigma_{22}(t)$ and $\sigma_{33}(t)$ have been evaluated in the same way.

3.3.2. Shear Stresses

Shear stresses are obtained in the same approach, the only difference is this time $i \neq j$.

$$\sigma_{ij,k+1} = G\gamma_{ij,k+1} + G_\beta \Delta t^{-\beta} \sum_{n=1}^{k+1} \mu_i^{(\beta)} \gamma_{ij,k-n+2} \quad , \quad i \neq j \quad (3.32)$$

3.4. Finite Element Implementation

3.4.1. UMAT Subroutine

ABAQUS/Standard involves an interface that provides an environment for the user to implement different constitutive equations. The developed material model will be implemented into user subroutine UMAT in ABAQUS/Standard. This interface allows any constitutive model with any complexity to be developed.

3.4.1.1. Steps Required in Writing a UMAT

In order to develop a UMAT subroutine, the appropriate description for the constitutive equation is needed to be done so by the explicit description of stress or the description of stress rate only. To get the incremental constitutive equation three methods are available, depending on the type of the problem one can be selected. One these methods is forward Euler. Forward Euler or explicit integration approaches of integration are easy but have a boundary of stability where it is generally less than the magnitude of the elastic stress. It should be noted that the time stepping has to be monitored for explicit integration. The algorithm is more complex for implicit or midpoint integration and often needs local iteration. Usually, though, there is no limit to stability.

To write the UMAT, the Jacobian matrix of the constitutive model should be calculated:

The coherent Jacobian for infinitesimal strain problems or finite strain problems with small volume changes.

$$C = \frac{\partial \Delta \sigma}{\partial \Delta \varepsilon} \quad (3.26)$$

where $\Delta \sigma$ stress increment and $\Delta \varepsilon$ is the strain increment. This matrix can be non-symmetric as a result of the constitutive equation or integration procedure. The variables which should be passed in for information and which should be calculated by the user in UMAT are available in ABAQUS's documentary.

3.5. Developing a UMAT Subroutine for FKV Model

In this section, the procedure of writing a UMAT code for fractional Kelvin-Voigt model will be explained. Using equation 3.31, the stress increment for the $k + 1^{st}$ increment will be:

$$\begin{aligned} \Delta \sigma_{11,k+1} = & K \Delta \varepsilon_{s,k+1} + 2G \Delta \varepsilon_{11,k+1} - \frac{2}{3} G \Delta \varepsilon_{s,k+1} \\ & + K_{\theta} \Delta t^{-\theta} \left[\sum_{n=1}^k \mu_n^{(\theta)} \Delta \varepsilon_{s,k-n+2} + \mu_{k+1}^{(\theta)} \Delta \varepsilon_{s,1} \right] \\ & - \frac{2}{3} G_{\beta} \Delta t^{-\beta} \left[\sum_{n=1}^k \mu_n^{(\beta)} \varepsilon_{s,k-n+2} + \mu_{k+1}^{(\beta)} \Delta \varepsilon_{s,1} \right] \\ & + 2G_{\beta} \Delta t^{-\beta} \left[\sum_{n=1}^k \mu_n^{(\beta)} \varepsilon_{11,k-n+2} + \mu_{k+1}^{(\beta)} \Delta \varepsilon_{11,1} \right] \end{aligned} \quad (3.34)$$

where,

$$\Delta \sigma_{11,k+1} = \sigma_{11,k+1} - \sigma_{11,k} \quad (3.27)$$

The other normal stress components will be evaluated in the UMAT by rotating the stress component indices. Consequently, only equation 3.34 was coded.

If $k = 0$, then,

$$\begin{aligned} \Delta\sigma_{11,1} = & K\Delta\varepsilon_{s,1} + 2G\Delta\varepsilon_{11,1} - \frac{2}{3}G\Delta\varepsilon_{s,1} + K_\theta\Delta t^{-\theta}[\mu_1^{(\theta)}\Delta\varepsilon_{s,1}] \\ & - \frac{2}{3}G_\beta\Delta t^{-\beta}[\mu_1^{(\theta)}\Delta\varepsilon_{s,1}] + 2G_\beta\Delta t^{-\beta}[\mu_1^{(\theta)}\Delta\varepsilon_{11,1}] \end{aligned} \quad (3.36)$$

$$\frac{\partial\Delta\sigma_{11,1}}{\partial\Delta\varepsilon_{11,1}} = K + K_\theta\Delta t^{-\theta}\mu_1^{(\theta)} + \frac{4}{3}G + \frac{4}{3}G_\beta\Delta t^{-\beta}\mu_1^{(\beta)} = A(1) \quad (3.28)$$

$$\frac{\partial\Delta\sigma_{11,1}}{\partial\Delta\varepsilon_{22,1}} = K + K_\theta\Delta t^{-\theta}\mu_1^{(\theta)} - \frac{2}{3}G - \frac{2}{3}G_\beta\Delta t^{-\beta}\mu_1^{(\beta)} = B(1) \quad (3.38)$$

$$\frac{\partial\Delta\sigma_{11,1}}{\partial\Delta\varepsilon_{33,1}} = K + K_\theta\Delta t^{-\theta}\mu_1^{(\theta)} - \frac{2}{3}G - \frac{2}{3}G_\beta\Delta t^{-\beta}\mu_1^{(\beta)} = B(1) \quad (3.39)$$

If this Jacobian matrix called $J(1)$, $\frac{\partial\Delta\sigma_{11,1}}{\partial\Delta\varepsilon_{11,1}}$, $\frac{\partial\Delta\sigma_{11,1}}{\partial\Delta\varepsilon_{22,1}}$ and $\frac{\partial\Delta\sigma_{11,1}}{\partial\Delta\varepsilon_{33,1}}$ are the j_{11} , j_{12} and the j_{13} components of that matrix respectively. The Jacobian will be a symmetric matrix:

$$J(1) = \begin{bmatrix} A(1) & B(1) & B(1) \\ B(1) & A(1) & B(1) \\ B(1) & B(1) & A(1) \end{bmatrix} \quad (3.40)$$

$$\text{StressIncrement} = J(1) * \text{StrainIncrement}(1) \quad (3.41)$$

The finite element software ABAQUS receives the evaluated Jacobian that has the meaning of tangent stiffness. By evaluating the inverse of this Jacobian matrix the tangent compliance will be obtained which will be used to calculate the next strain increment to give again to the UMAT for the next step.

If $k = 1$, then,

$$\Delta\sigma_{11,2} = K\Delta\varepsilon_{s,2} + 2G\Delta\varepsilon_{11,2} - \frac{2}{3}G\Delta\varepsilon_{s,2} \quad (3.42)$$

$$\begin{aligned} &+ K_{\theta}\Delta t^{-\theta} \left[\sum_{i=1}^1 \mu_i^{(\theta)} \Delta\varepsilon_{s,3-i} + \mu_2^{(\theta)} \Delta\varepsilon_{s,1} \right] \\ &- \frac{2}{3}G_{\beta}\Delta t^{-\beta} \left[\sum_{i=1}^1 \mu_i^{(\beta)} \varepsilon_{s,3-i} + \mu_2^{(\theta)} \Delta\varepsilon_{s,1} \right] \\ &+ 2G_{\beta}\Delta t^{-\beta} \left[\sum_{i=1}^1 \mu_i^{(\beta)} \varepsilon_{11,3-i} + \mu_2^{(\theta)} \Delta\varepsilon_{11,1} \right] \end{aligned}$$

$$\frac{\partial\Delta\sigma_{11,2}}{\partial\Delta\varepsilon_{11,1}} = K_{\theta}\Delta t^{-\theta}\mu_2^{(\theta)} + \frac{4}{3}G_{\beta}\Delta t^{-\beta}\mu_2^{(\beta)} = C(2) \quad (3.43)$$

$$\frac{\partial\Delta\sigma_{11,2}}{\partial\Delta\varepsilon_{22,1}} = K_{\theta}\Delta t^{-\theta}\mu_2^{(\theta)} - \frac{2}{3}G_{\beta}\Delta t^{-\beta}\mu_2^{(\beta)} = D(2) \quad (3.44)$$

$$\frac{\partial\Delta\sigma_{11,2}}{\partial\Delta\varepsilon_{33,1}} = K_{\theta}\Delta t^{-\theta}\mu_2^{(\theta)} - \frac{2}{3}G_{\beta}\Delta t^{-\beta}\mu_2^{(\beta)} = D(2) \quad (3.45)$$

$$J^*(2) = \begin{bmatrix} C(2) & D(2) & D(2) \\ D(2) & C(2) & D(2) \\ D(2) & D(2) & C(2) \end{bmatrix} \quad (3.46)$$

$$\begin{aligned} \text{StressIncrement} &= J(1) * \text{StrainIncrement}(2) + J^*(2) * \\ &\text{StrainIncrement}(1) \end{aligned} \quad (3.47)$$

If $k = 2$, then,

$$\Delta\sigma_{11,3} = K\Delta\varepsilon_{s,3} + 2G\Delta\varepsilon_{11,3} - \frac{2}{3}G\Delta\varepsilon_{s,3} \quad (3.48)$$

$$\begin{aligned} & + K_\theta\Delta t^{-\theta} \left[\sum_{i=1}^2 \mu_i^{(\theta)} \Delta\varepsilon_{s,4-i} + \mu_3^{(\theta)} \Delta\varepsilon_{s,1} \right] \\ & - \frac{2}{3}G_\beta\Delta t^{-\beta} \left[\sum_{i=1}^2 \mu_i^{(\beta)} \varepsilon_{s,4-i} + \mu_3^{(\beta)} \Delta\varepsilon_{s,1} \right] \\ & + 2G_\beta\Delta t^{-\beta} \left[\sum_{i=1}^2 \mu_i^{(\beta)} \varepsilon_{11,4-i} + \mu_3^{(\beta)} \Delta\varepsilon_{11,1} \right] \end{aligned}$$

$$\frac{\partial\Delta\sigma_{11,3}}{\partial\Delta\varepsilon_{11,1}} = K_\theta\Delta t^{-\theta} \mu_3^{(\theta)} + \frac{4}{3}G_\beta\Delta t^{-\beta} \mu_3^{(\beta)} = C(3) \quad (3.49)$$

$$\frac{\partial\Delta\sigma_{11,3}}{\partial\Delta\varepsilon_{22,1}} = K_\theta\Delta t^{-\theta} \mu_3^{(\theta)} - \frac{2}{3}G_\beta\Delta t^{-\beta} \mu_3^{(\beta)} = D(3) \quad (3.50)$$

$$\frac{\partial\Delta\sigma_{11,3}}{\partial\Delta\varepsilon_{33,1}} = K_\theta\Delta t^{-\theta} \mu_3^{(\theta)} - \frac{2}{3}G_\beta\Delta t^{-\beta} \mu_3^{(\beta)} = D(3) \quad (3.51)$$

$$J^*(3) = \begin{bmatrix} C(3) & D(3) & D(3) \\ D(3) & C(3) & D(3) \\ D(3) & D(3) & C(3) \end{bmatrix} \quad (3.52)$$

$$\text{StressIncrement} \quad (3.53)$$

$$\begin{aligned} & = J(1) * \text{StrainIncrement}(3) + J^*(2) \\ & * \text{StrainIncrement}(2) + J^*(3) * \text{StrainIncrement}(1) \end{aligned}$$

then,

$$\text{stressIncrement} \quad (3.54)$$

$$\begin{aligned}
 &= J(1) * \text{strainIncrement}(k + 1) + J^*(2) \\
 &* \text{strainIncrement}(k) + J^*(3) \\
 &* \text{strainIncrement}(k - 1) + J^*(4) \\
 &* \text{strainIncrement}(k - 2) + \dots
 \end{aligned}$$

By increasing k the stress increment for each time step will be calculated, the algorithm to write the Jacobian matrix in UMAT is presented in figure 3.3. The same procedure has been applied for the shear stresses. The related code has been written using Fortran 90, the most important problem during the coding is strain history. By defining a matrix at the beginning of the code the strain increments for each step were stored in the related column of it (figure 3.2).

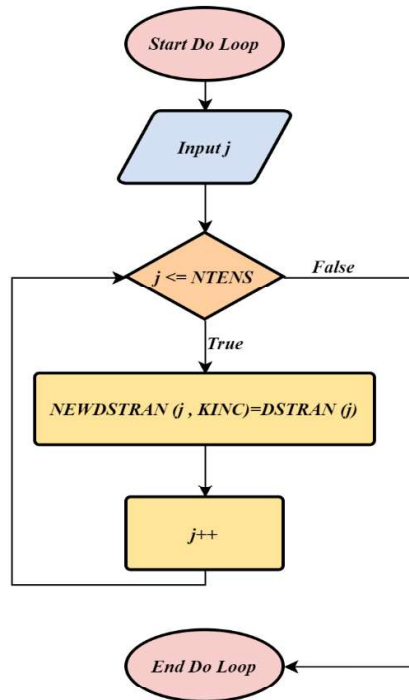


Figure 3.2. Flow chart for the Jacobian matrix.

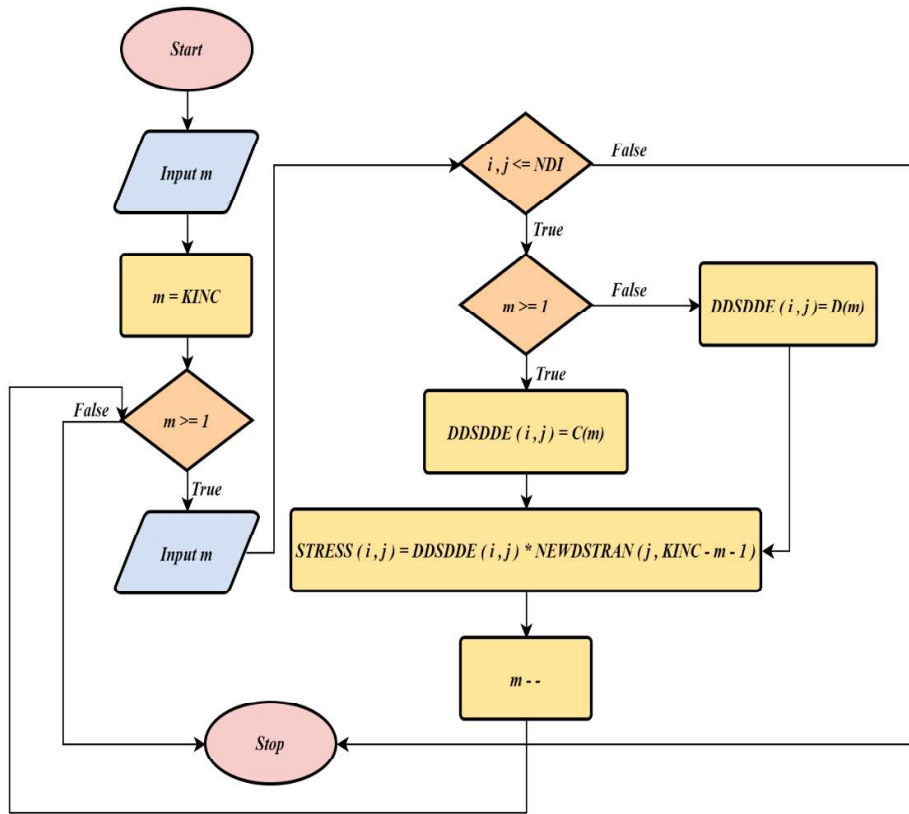


Figure 3.3. Flow chart for the strain history matrix.

3.6. Developing a UMAT Subroutine for Fractional Standard Linear Solid Model

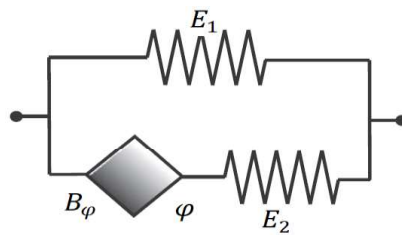


Figure 3.4. Fractional Standard Linear Solid Model.

In 2018 Alotta et al. claimed that equations 3.55 and 3.56 are capable of describing the behavior of the standard linear solid model (figure 3.4), but they did not report any numerical and theoretical solution to prove this claim. In this section these equations are expanded to be able to implement them in finite element code, on the other hand, numerical solution for these equations will be evaluated and the UMAT code will be written just like previous sections.

$$\sigma_{ii}^{k+1} = 2W_{\theta}^{k+1}\left(\varepsilon_{e,ii}, \frac{\sigma_{e,ii}}{2}\right) + 3W_{\theta}^{k+1}\left(\varepsilon_s, \frac{1}{3}\sigma_s\right); \quad i = 1,2,3; \quad (3.55)$$

$$\sigma_{ij}^{k+1} = W_{\theta}^{k+1}(\gamma_{ij}, \sigma_{ij}); \quad i \neq j; \quad (3.56)$$

where,

$$\varepsilon_{e,ii} = \varepsilon_{ii} - \frac{1}{3}\varepsilon_s \quad (3.29)$$

$$W_{\theta}^{k+1}(\varepsilon, \sigma) = \frac{E_1 E_2 + (E_1 + E_2)B_{\varphi}\Delta t^{-\varphi}}{E_2 + B_{\varphi}\Delta t^{-\varphi}} \varepsilon^{k+1} \quad (3.58)$$

$$+ \frac{E_{\varphi}\Delta t^{-\varphi}}{E_2 + E_{\varphi}\Delta t^{-\varphi}} \sum_{n=2}^{k+1} \mu_n^{(\varphi)} [(E_1 + E_2)\varepsilon^{k-n+2} - \sigma^{k-n+2}]$$

The equation 3.55 has been expanded in equation 3.58 for $i = 1$.

$$\begin{aligned}
\sigma_{11,k+1} = & \frac{4}{3}P_\beta \left(\varepsilon_{11,k+1} - \frac{\varepsilon_{22,k+1} + \varepsilon_{33,k+1}}{2} \right) & (3.59) \\
& + \frac{2}{3}T_\beta \sum_{n=2}^{k+1} \mu_n^{(\beta)} 2(G_1 \\
& + G_2) \left(\varepsilon_{11,k-n+2} - \frac{\varepsilon_{22,k-n+2} + \varepsilon_{33,k-n+2}}{2} \right) \\
& - \left(\sigma_{11,k-n+2} - \frac{\sigma_{22,k-n+2} + \sigma_{33,k-n+2}}{2} \right) + P_\theta \varepsilon_{s,k+1} \\
& + T_\theta \sum_{n=2}^{k+1} \mu_n^{(\theta)} \left((K_1 + K_2) \varepsilon_{s,k-n+2} - \frac{1}{3} \sigma_{sk-n+2} \right)
\end{aligned}$$

where,

$$P_\beta = \frac{G_1 G_2 + (G_1 + G_2) G_\beta \Delta t^{-\beta}}{G_2 + G_\beta \Delta t^{-\beta}} \quad (3.60)$$

$$P_\theta = \frac{K_1 K_2 + (K_1 + K_2) K_\theta \Delta t^{-\theta}}{K_2 + K_\theta \Delta t^{-\theta}} \quad (3.61)$$

$$T_\beta = \frac{G_\beta \Delta t^{-\beta}}{G_2 + G_\beta \Delta t^{-\beta}} \quad (3.62)$$

$$T_\theta = \frac{K_\theta \Delta t^{-\theta}}{K_2 + K_\theta \Delta t^{-\theta}} \quad (3.63)$$

The stress increment at $k + 1^{st}$ increment presented in equation 3.64.

The same procedure is used for deriving the finite element code for shear stress. The procedure of extracting the Jacobian for each increment is as same the method which has been used for fractional Kelvin-Voigt model. The only difference is that for the FKV model only a history for strains existed but for the fractional standard linear solid model the constitutive equation includes both the strain and stress history. To tackle

this problem another matrix for stress increments were defined the same as the strain increments in FKV model. The results and also the analytical solutions for both models are presented in the next chapter.

$$\begin{aligned}
\Delta\sigma_{11,k+1} = & \frac{4}{3}P_\beta \left(\Delta\varepsilon_{11,k+1} - \frac{\Delta\varepsilon_{22,k+1} + \Delta\varepsilon_{33,k+1}}{2} \right) & (3.30) \\
& + \frac{2}{3}T_\beta \left[\sum_{n=2}^k \mu_n^{(\beta)} 2(G_1 + G_2) \left(\Delta\varepsilon_{11,k-n+2} \right. \right. \\
& - \frac{\Delta\varepsilon_{22,k-n+2} + \Delta\varepsilon_{33,k-n+2}}{2} \left. \left. \right) - \left(\Delta\sigma_{11,k-n+2} \right. \right. \\
& - \frac{\Delta\sigma_{22,k-n+2} + \Delta\sigma_{33,k-n+2}}{2} \left. \left. \right) \right. \\
& + \mu_{k+1}^{(\beta)} \left(2(G_1 + G_2) \left(\Delta\varepsilon_{11,1} - \frac{\Delta\varepsilon_{22,1} + \Delta\varepsilon_{33,1}}{2} \right) \right. \\
& \left. \left. - \left(\Delta\sigma_{11,1} - \frac{\Delta\sigma_{22,1} + \Delta\sigma_{33,1}}{2} \right) \right) \right] + P_\theta \Delta\varepsilon_{s,k+1} \\
& + T_\theta \left[\sum_{n=2}^k \mu_n^{(\theta)} \left((K_1 + K_2) \Delta\varepsilon_{s,k-n+2} - \frac{1}{3} \Delta\varepsilon_{sk-n+2} \right) \right. \\
& \left. + \mu_{k+1}^{(\theta)} \left((K_1 + K_2) \Delta\varepsilon_{s,1} - \frac{1}{3} \Delta\sigma_{s,1} \right) \right]
\end{aligned}$$

CHAPTER 4

RESULTS AND DISCUSSION

4.1. Fractional Kelvin-Voigt (FKV) Model

The Fortran code for the equation 3.34 has been developed and linked to the finite element software ABAQUS/Standard. The code has been run for the relaxation and creep tests for a single element. The element type was C3D8 for a cube (figure 4.1), the size of the cube was 1 mm^3 . The code was run for 10 seconds with an adaptive $\Delta t = 0.01 \text{ sec}$. The duration of the analysis was about 15 minutes which was not too long for an ordinary laptop with the installed memory RAM of 16 GB. Also the computational results were compared to the analytical outcomes which will be explained in the following pages.

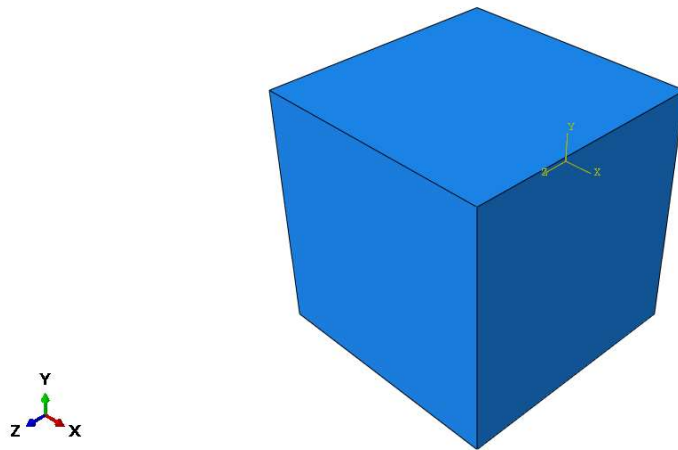


Figure 4.1. The single element in the ABAQUS software.

4.1.1. Analytical Solution

The boundary conditions applied for the analytical solution is as below:

$$\varepsilon_{11}(t) = \bar{\varepsilon}(tU(t) + U(t-1)(1-t)) \quad (4.1)$$

$$\varepsilon_{22}(t) = \varepsilon_{33}(t) = 0 \quad (4.2)$$

$U(t)$ is the step function.

By substituting equations 3.27 and 3.28 into the Boltzmann superposition formula, and using equation 4.1 the equation below for the stress in the direction which displacement was applied which is the relaxation function will be obtained (considering that the orders of bulk and shear power laws are equal ($\theta = \beta$)):

$$\begin{aligned} \sigma_{11}(t) = \bar{\varepsilon} \left\{ \left[\left(\frac{4}{3} G_{\beta} + K_{\beta} \right) \frac{t^{(1-\beta)}}{\Gamma(2-\beta)} + \left(\frac{4}{3} G + K \right) t \right] U(t) \right. \\ \left. - \left[\left(\frac{4}{3} G_{\beta} + K_{\beta} \right) \frac{(t-1)^{(1-\beta)}}{\Gamma(2-\beta)} + \left(\frac{4}{3} G + K \right) (t-1) \right] U(t-1) \right\} \end{aligned} \quad (4.3)$$

where $\bar{\varepsilon} = 0.01$ and the other material constants are available in table 4.1.

Table 4.1. Material parameters which used for fractional Kelvin-Voigt model (Alotta et al., 2018).

Material Parameter	Value	Unit
K	1000	MPa
G	750	MPa
$K_{\theta} = K_{\beta}$	500	MPa sec ^{θ}
G_{β}	375	MPa sec ^{θ}

To obtain the analytical result for the fractional Kelvin-Voigt model equation 4.3, has been plotted using MATLAB software (figure 4.3).

4.1.2. Computational Results

For $\beta = 0.3$ the analytical results have been compared to the computational graph (figure 4.3). The boundary conditions applied for the finite element approach is the same as analytical approach in which a single element has been considered. The displacement which was applied to one face of the cube in the x direction was 0.01 of its original length and the opposite face restricted in all directions. The displacement was applied as a ramp for one second and then it remained constant for 9 seconds (figure 4.2). As shown in the figure both results fit each other very good, which is a verification of the UMAT code.

The different behavior of this model by changing the value of the fractional coefficient is possible. In figure 4.4 those behaviors for $\theta = \beta = 0, 0.25, 0.5, 0.75, 1$ are shown. As it is obvious as the amount of β increases the rubbery behavior of the model increases as well and as it decreases the glassy behavior of the material decreases.

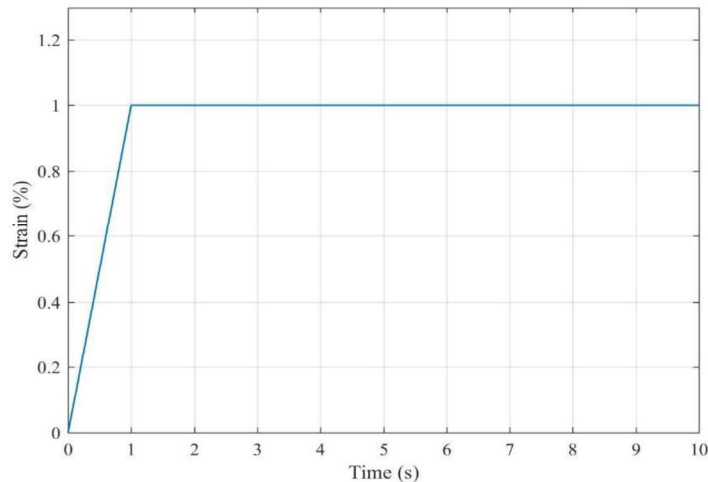


Figure 4.2. Strain history during the relaxation test (the strain in the curve is ε_{11}).

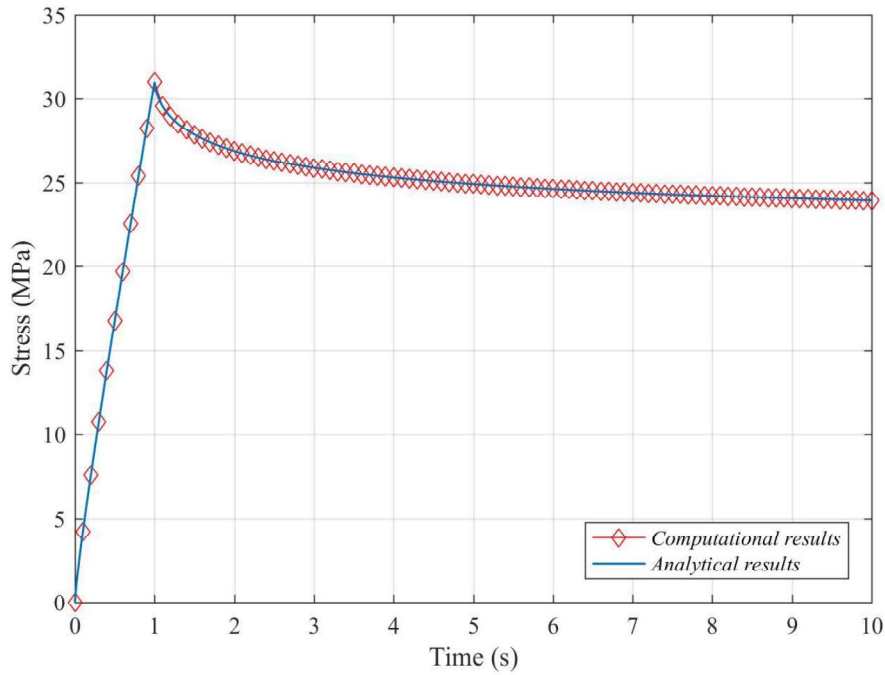


Figure 4.3. Comparison between analytical and computational results for the relaxation test for the fractional Kelvin-Voigt model (the stress in the curve is σ_{11}).

When the fractional coefficient be one, the fractional Kelvin-Voigt model turns into the classical Kelvin-Voigt model (with dashpot). The behavior of the model under this condition is shown in figure 4.4. Another simulation which analyzed for this model was the creeping test. This time the total stress of 10 MPa was applied to one face of the cube and the opposite face was constrained in the direction which stress applied (figure 4.5). The computational results for the creep test for different fractional coefficients are shown in the figure 4.6 and figure 4.7.

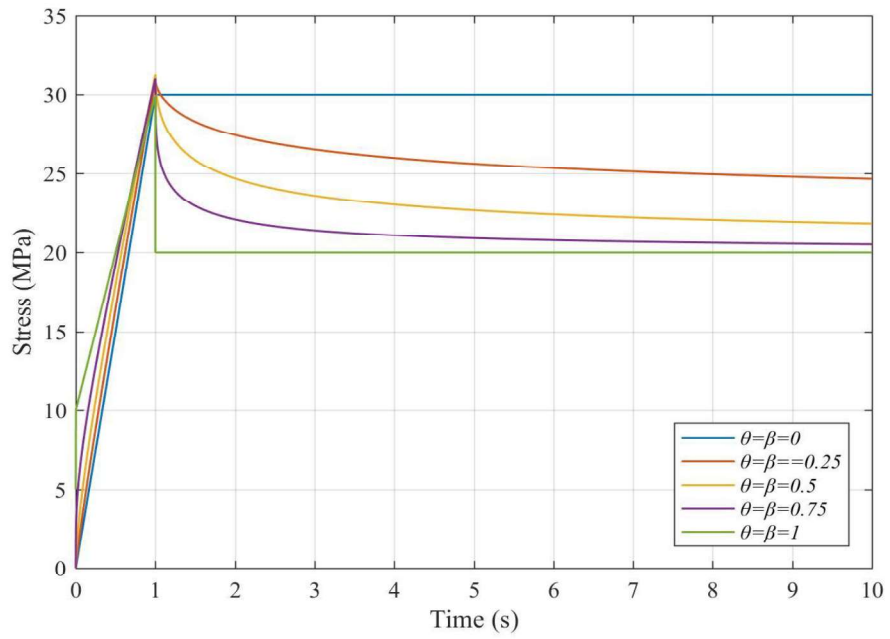


Figure 4.4. Different behavior of the fractional Kelvin-Voigt model for relaxation test for different values of fractional coefficient (the stress in the curve is σ_{11}).

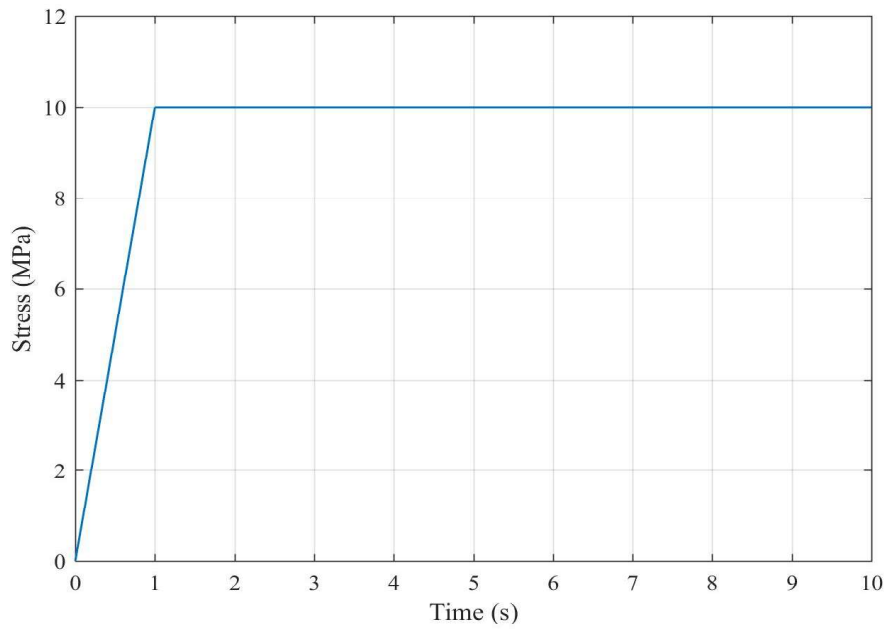


Figure 4.5. Stress history during the creep test (the stress in the curve is σ_{11}).

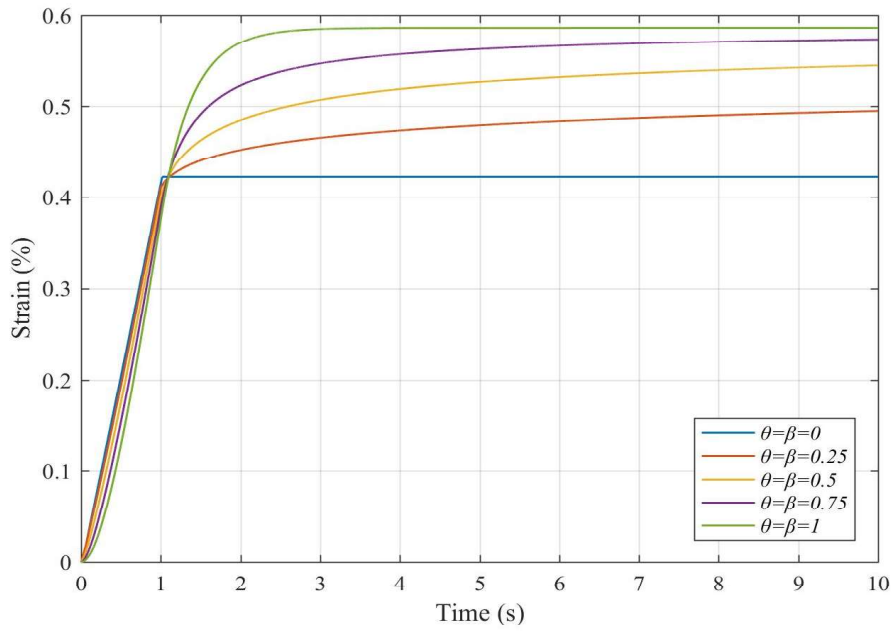


Figure 4.6. Different behavior of the fractional Kelvin-Voigt model for creep test for different values of fractional coefficient (the strain in the curve is ϵ_{11}).

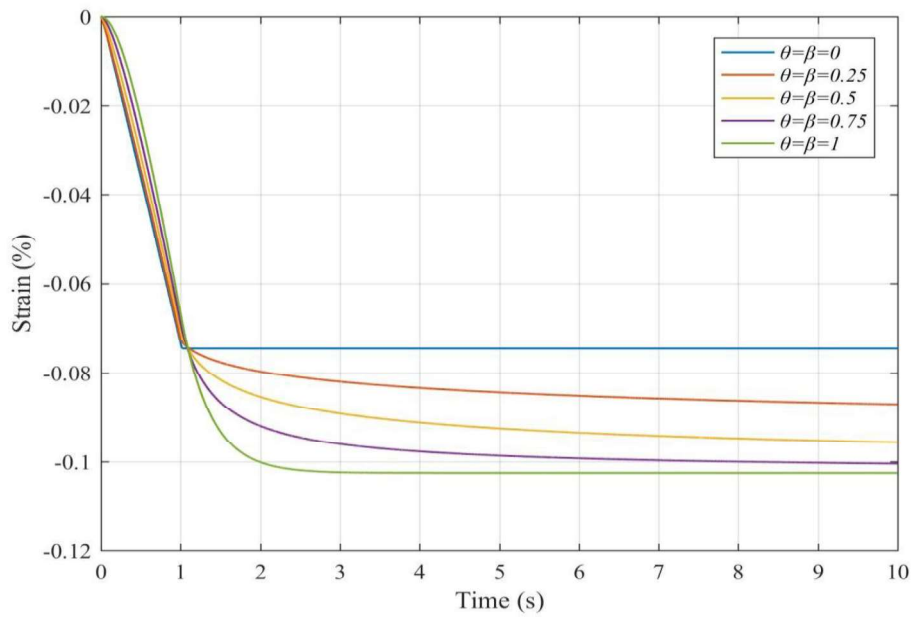


Figure 4.7. Different behavior of the fractional Kelvin-Voigt model for creep test for different values of fractional coefficient (the strain in the curve is $\epsilon_{22} = \epsilon_{33}$).

4.2. Single Fractional Element (Spring-Pot)

By considering the relaxation function of a single spring-pot (equation 4.4) the deviatoric and volumetric relaxation functions will be obtained (equations 4.5 and 4.6).

$$R(t) = \frac{B_\varphi t^{-\varphi}}{\Gamma(1-\varphi)} \quad (4.4)$$

then,

$$K_R(t) = \frac{K_\theta t^{-\theta}}{\Gamma(1-\theta)} \quad (4.5)$$

$$G_R(t) = \frac{G_\beta t^{-\beta}}{\Gamma(1-\beta)} \quad (4.31)$$

By substituting the deviatoric and volumetric relaxation functions in the Boltzmann superposition principle the following constitutive equation for a single spring-pot will be obtained:

$$\begin{aligned} \sigma_{11,k+1} = & \frac{K_\theta}{\Gamma(1-\theta)} \int_0^t (t-\tau)^{-\theta} \dot{\epsilon}_{s,k+1} d\tau \\ & - \frac{2}{3} \frac{G_\beta}{\Gamma(1-\beta)} \int_0^t (t-\tau)^{-\beta} \dot{\epsilon}_{s,k+1} d\tau \\ & + 2 \frac{G_\beta}{\Gamma(1-\beta)} \int_0^t (t-\tau)^{-\beta} \dot{\epsilon}_{11,k+1} d\tau \end{aligned} \quad (4.7)$$

By looking at equation 4.7 and equation 3.29 it can be conducted that by taking K and G , as zero in the equation 3.29 the equation 4.7 will be evaluated.

Therefore, instead of generating a new code for the fractional element by taking G and K in the FORTRAN code of the fractional Kelvin-Voigt the behavior of the spring-

pot can be simulated easily. The boundary conditions are the same as fractional Kelvin-Voigt model. The computational results for this model which present the relaxation and creep tests are shown in figures 4.8, 4.9 and 4.10.

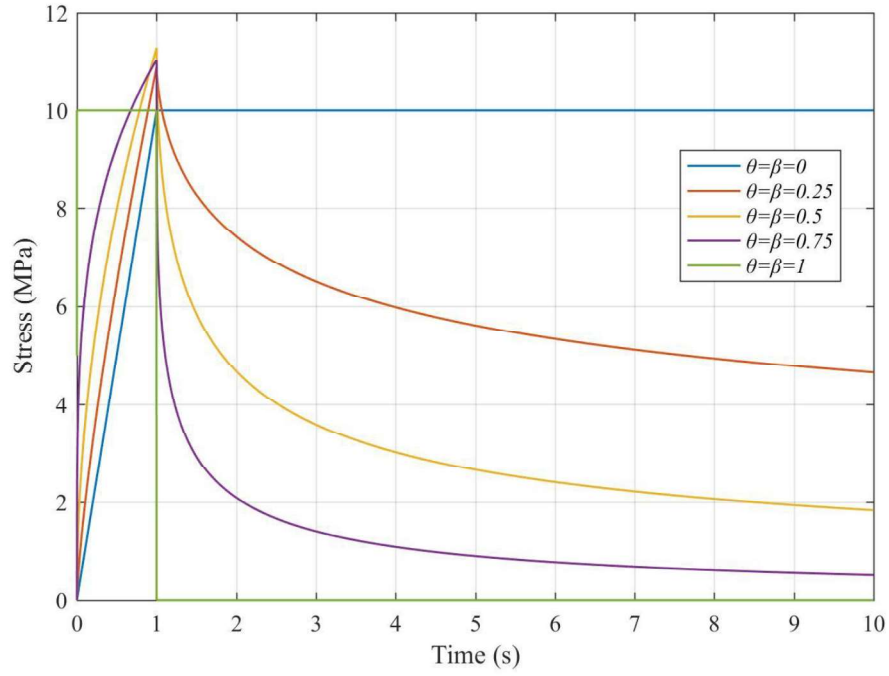


Figure 4.8. Different behavior of the single spring-pot for the relaxation test for different values of fractional coefficient (the stress in the curve is σ_{11}).

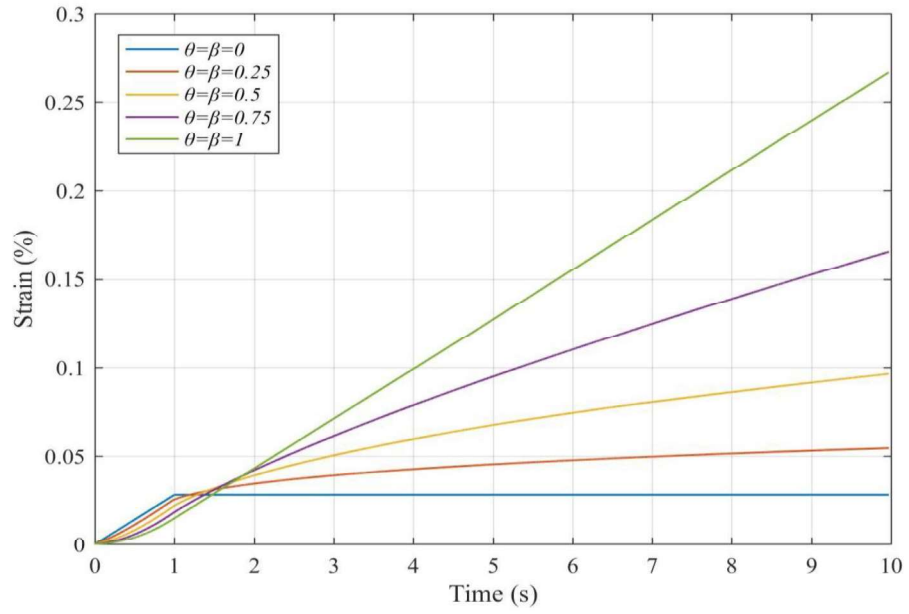


Figure 4.9. Different behavior of the single spring-pot for creep test for different values of fractional coefficient (the strain in the curve is ϵ_{11}).

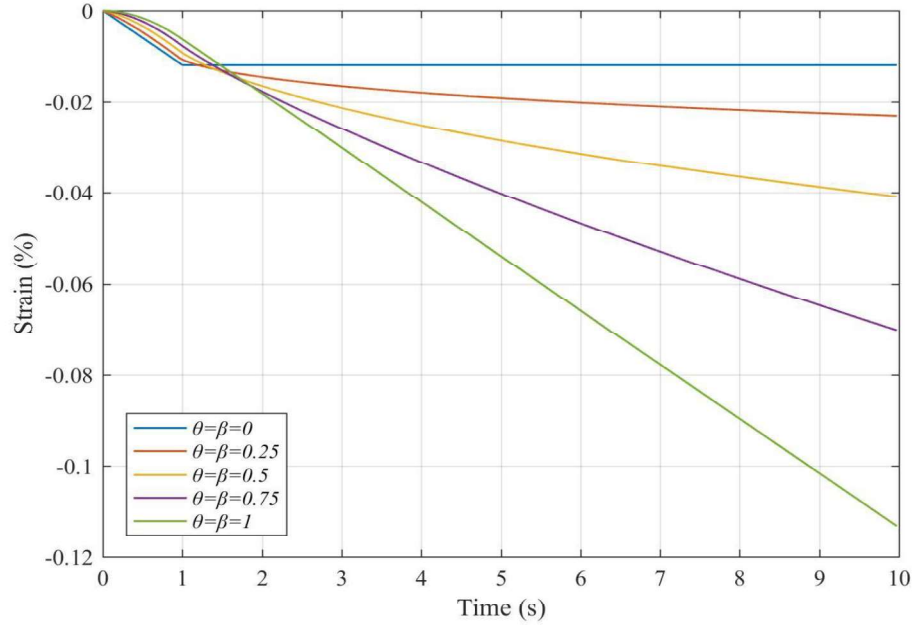


Figure 4.10. Different behavior of the single spring-pot for creep test for different values of fractional coefficient (the strain in the curve is $\epsilon_{22} = \epsilon_{33}$).

4.3. Fractional Standard Linear Solid Model

4.3.1. Analytical Solution

For a fractional standard linear solid model, the relaxation function is given as:

$$R(t) = E_1 + E_2 E_\varphi \left(-\frac{E_2}{E_\varphi} t^\varphi \right) \quad (4.32)$$

therefore its volumetric ($K_R(t)$) and deviatoric ($G_R(t)$) parts will be written as:

$$K_R(t) = K_1 + K_2 E_\theta \left(-\frac{K_2}{K_\theta} t^\theta \right) \quad (4.9)$$

$$G_R(t) = G_1 + G_2 E_\beta \left(-\frac{G_2}{G_\beta} t^\beta \right) \quad (4.10)$$

a strain history (equation 4.1) for $\beta = \theta$ was applied as one of the boundary conditions and $\varepsilon_{22}(t) = \varepsilon_{33}(t) = 0$. Using these equations and the Boltzmann superposition with the same procedure which has been taken for the analytical solution of the fractional Kelvin-Voigt model the stress at the direction which displacement applied will be gained (equation 4.11).

$$\begin{aligned} \sigma_{11}(t) = \bar{\varepsilon} \left\{ \left[K_1 + K_2 E_{\beta,2} \left(-\frac{K_2}{K_\beta} t^\beta \right) \right. \right. & \quad (4.11) \\ & + \left. \frac{4}{3} \left(G_1 + G_2 E_{\beta,2} \left(-\frac{G_2}{G_\beta} t^\beta \right) \right) \right] t U(t) \\ & - \left[K_1 + K_2 E_{\beta,2} \left(-\frac{K_2}{K_\beta} (t-1)^\beta \right) \right. \\ & \left. \left. + \frac{4}{3} \left(G_1 + G_2 E_{\beta,2} \left(-\frac{G_2}{G_\beta} (t-1)^\beta \right) \right) \right] (t-1) U(t-1) \right\} \end{aligned}$$

where $E_{\alpha,\beta}(Z)$ is the two parameter Mittag-Leffler function. Equation 4.11 has been plotted in MATLAB using parameters in table 4.2 as the analytical solution for the fractional standard linear solid mode (figure 4.11).

Table 4.2. *Material parameters used for fractional standard linear solid model (Alotta et al., 2018).*

Material Parameter	Value	Unit
K_1	1000	MPa
K_2	500	MPa
G_1	750	MPa
G_2	375	MPa
$K_\theta = K_\beta$	500	MPa sec ^{θ}
G_β	375	MPa sec ^{θ}

4.3.2. Computational Results

The equation 4.11 was plotted in MATLAB using the function which developed by Igor Podlubny for Mittag-Leffler function in this software (MATLAB and Statistics Toolbox Release 2016b). and the computational and analytical results were compared in Figure 4.11. The element type was C3D8 and since for this model both strain and stress histories are needed the duration of analysis was about 30 minutes which is double the analysis time needed for the fractional Kelvin-Voigt in which only the strain history is required. Both fractional coefficients were taken as 0.3. Based on figure 4.10 the results from the analytical approach and the finite element approach are in a good agreement with each other which is a verification for the UMAT. The behavior of this model for the relaxation and creep tests with the same strain and stress histories (figures 4.2 and 4.5) are shown in figures 4.12, 4.13 and 4.14.

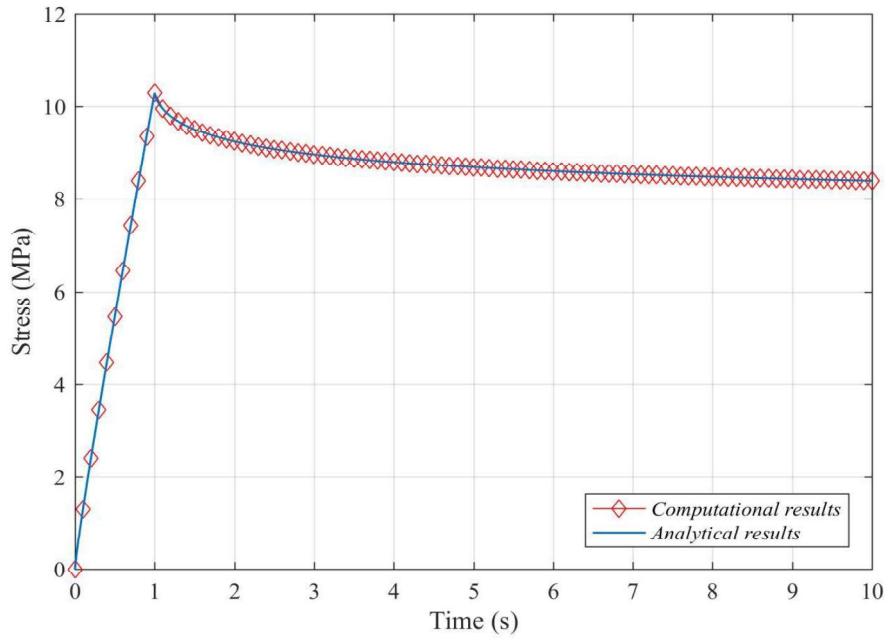


Figure 4.11. Comparison between analytical and computational results for the relaxation test for the fractional standard linear solid model (the stress in the curve is σ_{11}).

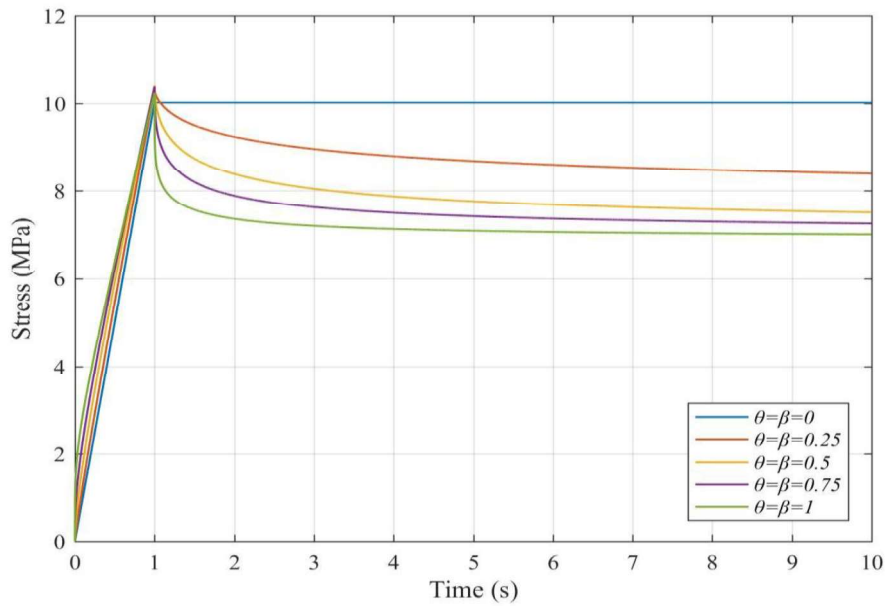


Figure 4.12. Different behavior of the fractional standard linear solid model for the relaxation test for different values of fractional coefficient (the stress in the curve is σ_{11}).

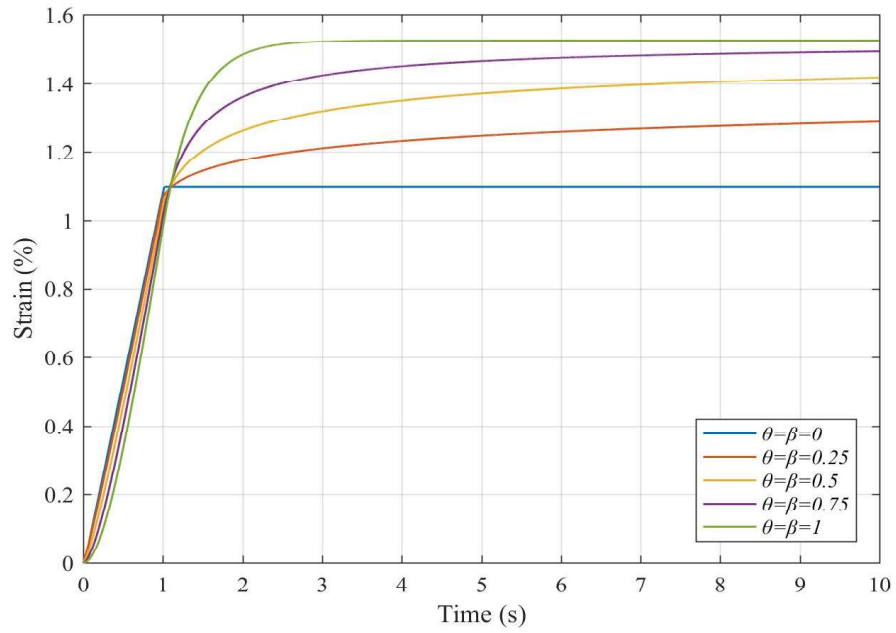


Figure 4.13. Different behavior of the fractional standard linear solid model for creep test for different values of fractional coefficient (the strain in the curve is ϵ_{11}).

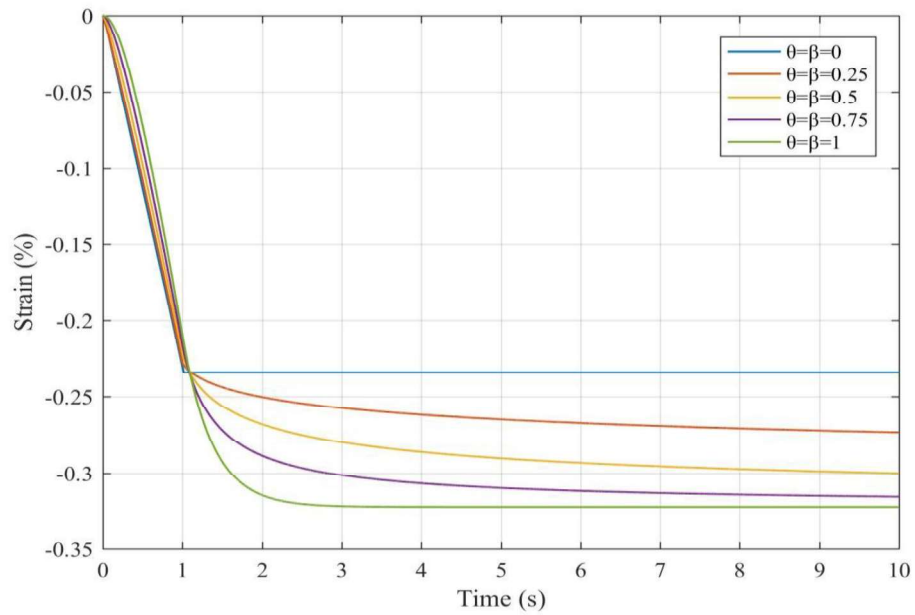


Figure 4.14. Different behavior of the fractional standard linear solid model for creep test for different values of fractional coefficient (the strain in the curve is $\epsilon_{22} = \epsilon_{33}$).

To determine the behavior of the coded model under different circumstances a different strain history and stress history are applied with a different amplitude (figures 4.15 and 4.16). The computational outcomes for relaxation and creep tests for fractional Kelvin-Voigt and fractional standard linear solid models are shown in figures 4.17 and 4.18, 4.19, 4.20, 4.21 and 4.22.

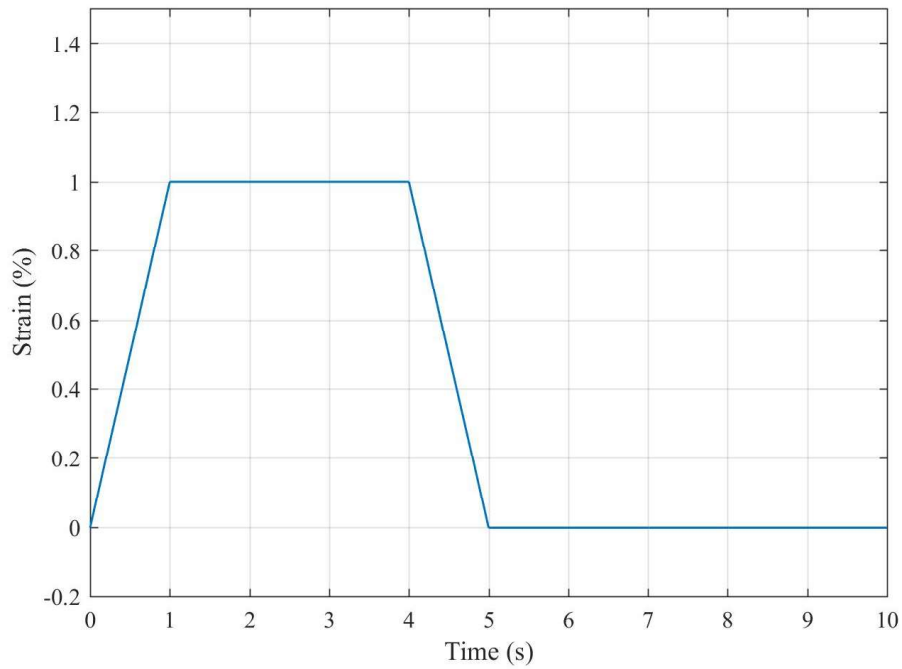


Figure 4.15. Strain history during the relaxation test (the strain in the curve is ε_{11}).

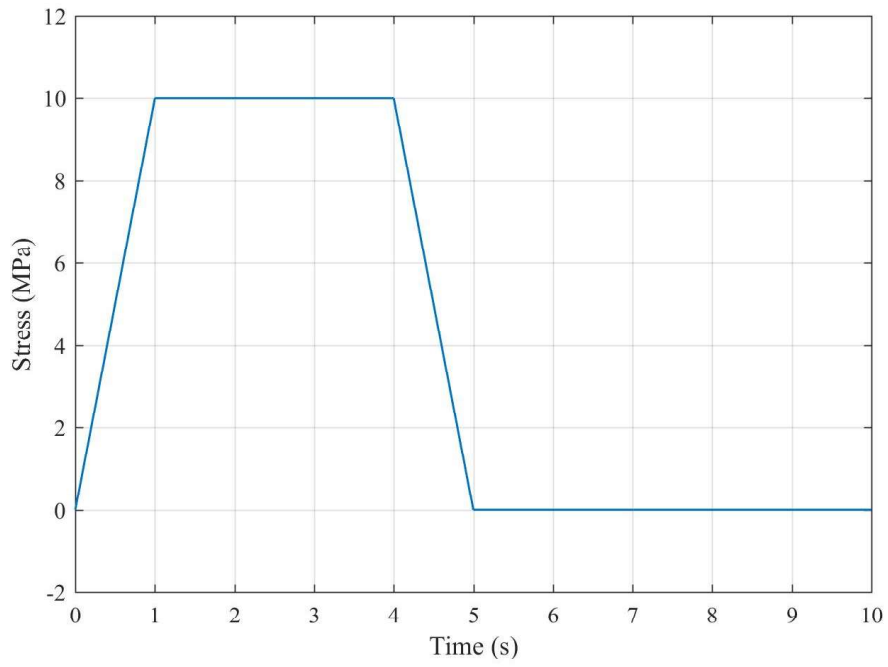


Figure 4.16. Stress history during the creep test (the stress in the curve is σ_{11}).

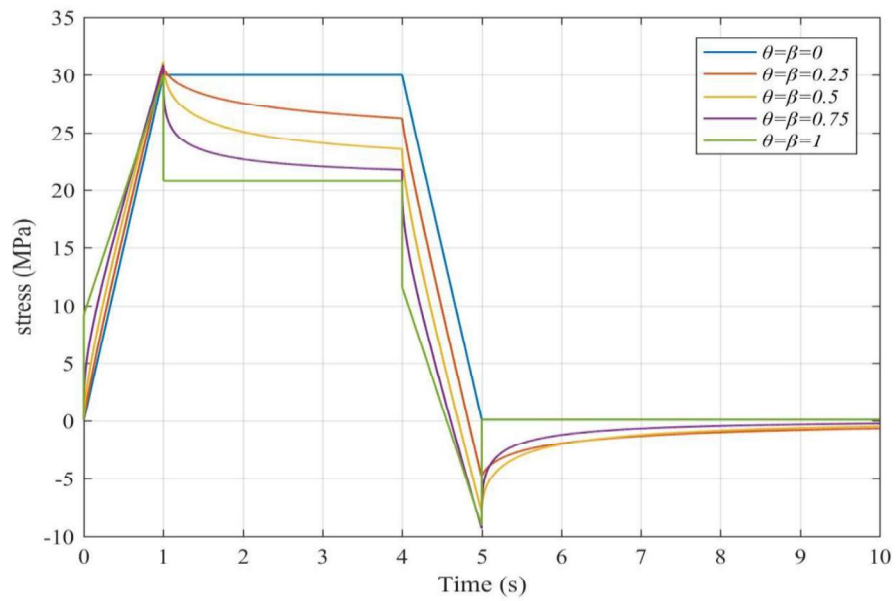


Figure 4.17. Different behavior of the fractional Kelvin-Voigt model for the relaxation test for different values of fractional coefficient (the stress in the curve is σ_{11}).

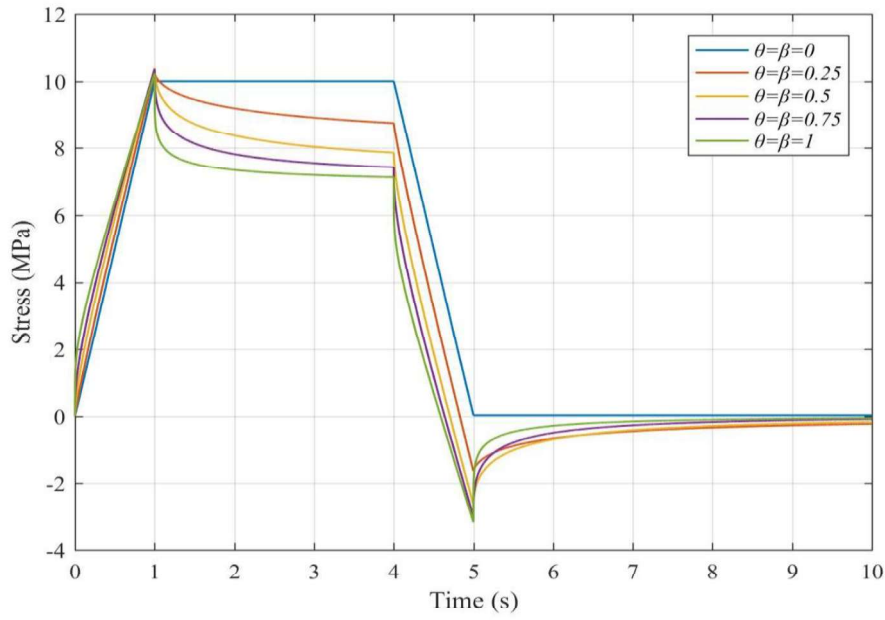


Figure 4.18. Different behavior of the fractional standard linear solid model for the relaxation test for different values of fractional coefficient (the stress in the curve is σ_{11}).

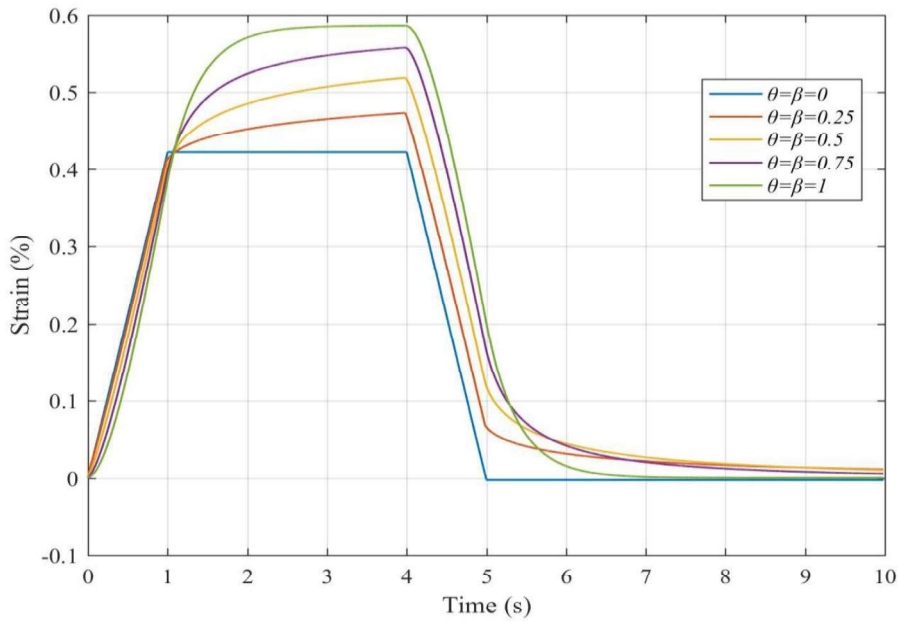


Figure 4.19. Different behavior of the fractional Kelvin-Voigt model for creep test for different values of fractional coefficient (the strain in the curve is ϵ_{11}).

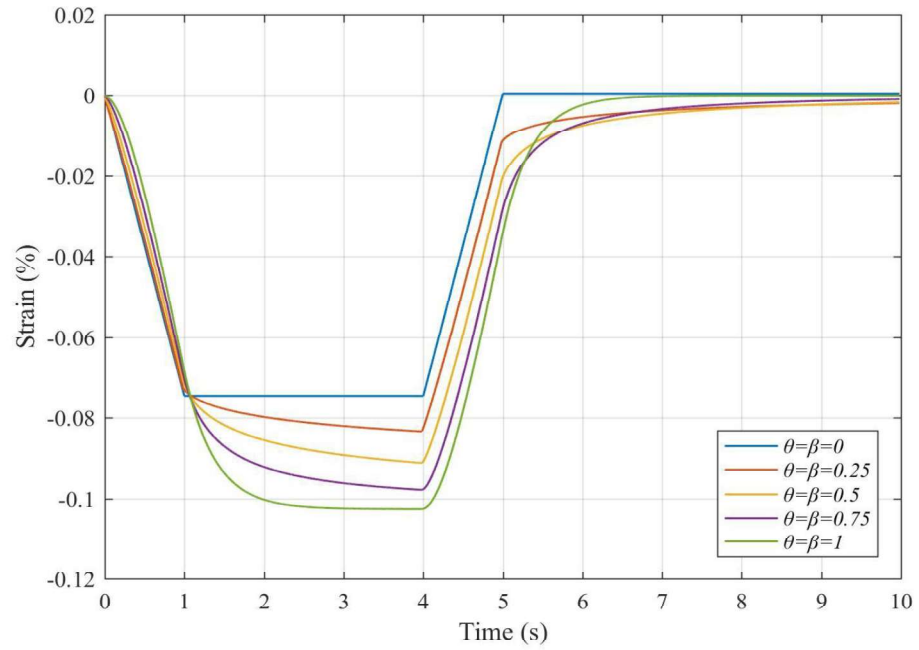


Figure 4.20. Different behavior of the fractional Kelvin-Voigt model for creep test for different values of fractional coefficient (the strain in the curve is $\varepsilon_{22} = \varepsilon_{33}$).

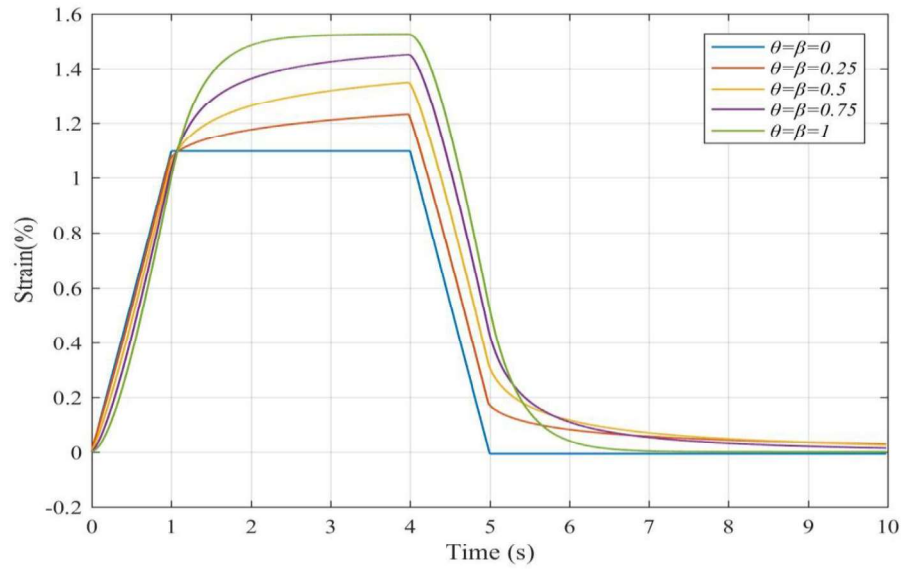


Figure 4.21. Different behavior of the fractional standard linear solid model for creep test for different values of fractional coefficient (the strain in the curve is ε_{11}).

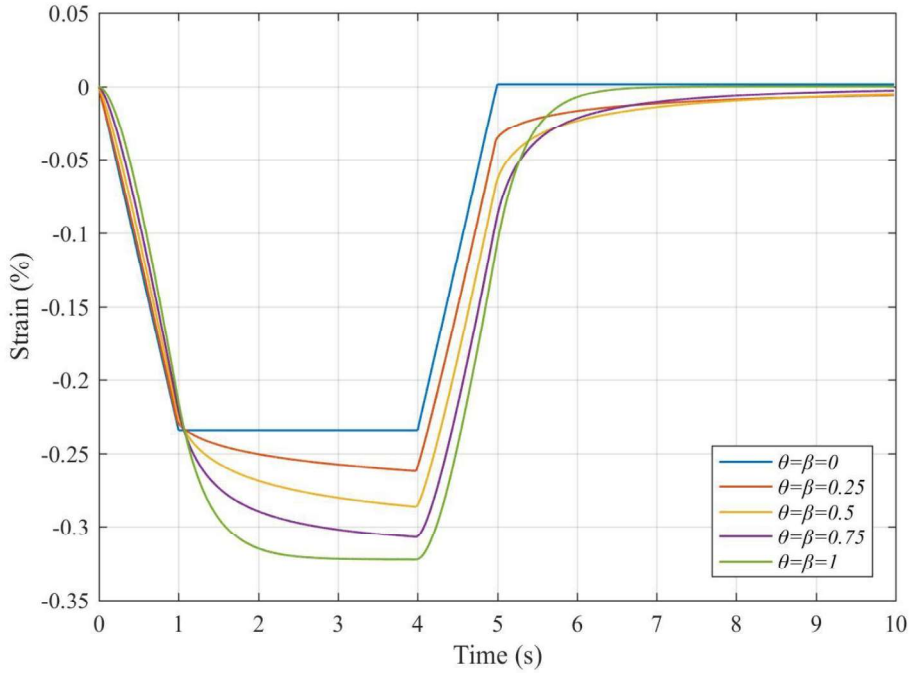


Figure 4.22. Different behavior of the fractional standard linear solid model for creep test for different values of fractional coefficient (the strain in the curve is $\varepsilon_{22} = \varepsilon_{33}$).

The analytical outcomes fitted the theoretical results for all material models well. It has been shown that stress will increase through relaxation testing by raising the strain. The material model starts relaxing when the strain starts to stay constant and in this case the real behavior of a viscoelastic model during the relaxation tests was well simulated. During the creep test when the stress increases the strain in the direction which the stress has been applied (ε_{11}) increases as well then the applied stress began to stay constant and the model started to creep. Due to the poisson effect the strains in the other directions (ε_{22} and ε_{33}) started to decrease by increasing the stress .There is one thing in common between all of the graphs represented in this chapter. In all of them increasing the fractional coefficient makes spring-pot less elastic and more viscous therefore, it is possible to see the smooth transition between elastic and viscous behavior just by changing the fractional coefficients. Also, it has been showed

that although the classical Kelvin-Voigt model (figure 4.4, when $\theta = \beta = 1$) cannot demonstrate the real material behaviors but with the fractional form of it is possible to develop real behavior of materials (figure 4.4, when $\theta = \beta < 1$). Utilizing this approach viscoelastic models can be developed which demonstrates the material behavior for any stages of rubbery and glassy conduct which is an advantage in comparison to classical viscoelastic material models. On the other hand, classical viscoelastic material models are a special case of this approach ($\beta = \theta = 1$).

CHAPTER 5

CONCLUSION AND RECOMMENDATIONS FOR FUTURE STUDIES

5.1. Conclusion and Discussion

In this study isotropic 3-D fractional constitutive models utilizing linear viscoelasticity theory have been developed for the fractional Kelvin-Voigt and the fractional standard linear solid models. The application of Boltzmann superposition principle has been demonstrated throughout this work. The discretized form of the fractional derivative generated by Grünwald-Letnikov were used to evaluate the numerical solutions of the constitutive models to be able to implement them in ABAQUS/Standard.

The related fractional constitutive models have been implemented into FE software ABAQUS/Standard using the UMAT routine. Although the proposed material models are capable of using in simulation of finite strain but the verification has been done only for small strain to simplify the analytical solution. In this study the user defined subroutine has been generated using the Jacobian matrix not the strain energy density function. By comparing the results obtained using finite element approach for relaxation and creep tests with the analytical methods for a single element, it was shown that the derived constitutive models are capable of simulating the real response of a linear viscoelastic body successfully. Based on the results related to the fractional Kelvin-Voigt model the ability of this model in predicting real behavior of the viscoelastic materials in comparison with the classical model has been demonstrated. The most important difficulty during the coding was the hereditary dependency of the models which means the strain and stress history. It was shown that for the fractional Kelvin-Voigt model only the strain history is required while for the fractional standard linear solid model besides the strain history, a history for stresses is needed at the same time. This problem has been tackled by defining matrices for stresses and strains. All

stress and strain increments for every time step were stored in the related column of these matrices. The models presented in this work can simulate the response of the viscoelastic materials by changing the fractional coefficient from glassy to rubbery. Also, the behavior of a single spring pot (fractional element) was simulated using the FKV's routine by changing the amount of variables easily. The number of material constants which appeared in the constitutive equations of the standard linear solid model is seven parameters which is considerably lower than the proposed equations which evaluated using other methods (nine parameters using the strain energy density function), which can be so beneficial in case of extracting material parameters using experimental data. Also, it has been demonstrated that the stress and strain history for each fractional viscoelastic model at each Gauss point of each component is accessible as column matrices which is crucial for the positive implementation of the model. This research shows that it is possible to implement 3D fractional viscoelastic models into FE software, easily and efficiently.

5.2. Future Studies

There are some works which can be done in the future:

- 1- The first work that can be done in the development of multi-element subroutine codes. It can also be done by using better workstations by using a special file to store the stress and stress history instead of the matrices, the amount of memory required can be significantly reduced.
- 2- These findings can be used to obtain material parameters by fitting the experimental results to the relaxation and creep tests.
- 3- All the assumptions taken in this research are based on the condition of isotropy. Another work can be an assessment of the constitutive 3-D anisotropic models that will be simulated by using more materials and their behaviors.
- 4- In determining material features, temperature is a significant parameter. UMAT subroutines can therefore be created by taking into account this issue

using the matrix called $DDSDDT(NTENS)$, which is the variation of the temperature-related stress increments.

REFERENCES

- Adolfsson, K., Enelund, M., & Olsson, P. (2005). On the fractional order model of viscoelasticity. *Mechanics of Time-dependent materials*, 9(1), 15-34.
- Ahn, B., & Kim, J. (2009). Efficient soft tissue characterization under large deformations in medical simulations. *International Journal of Precision Engineering and Manufacturing*, 10(4), 115-121.
- Alotta, G., Barrera, O., Cocks, A., & Di Paola, M. (2018). The finite element implementation of 3D fractional viscoelastic constitutive models. *Finite Elements in Analysis and Design*, 146, 28-41.
- Bernstein, B., Kearsley, E. A., & Zapas, L. J. (1963). A study of stress relaxation with finite strain. *Transactions of the Society of Rheology*, 7(1), 391-410.
- Biot, M. A. (1965). *Mechanics of incremental deformations*.
- Blair, G. S. (1944). Analytical and integrative aspects of the stress-strain-time problem. *Journal of Scientific Instruments*, 21(5), 80.
- Blair, G. W. S., & Copen, F. M. V. (1939). The subjective judgement of the elastic and plastic properties of soft bodies; the " differential thresholds" for viscosities and compression moduli. *Proceedings of the Royal Society of London. Series B-Biological Sciences*, 128(850), 109-125.
- Bland, D. R. (2016). *The theory of linear viscoelasticity*. Courier Dover Publications.
- Burnham, K. P., & Anderson, D. R. (2002). A practical information-theoretic approach. *Model selection and multimodel inference, 2nd ed.* Springer, New York.
- Christensen, R. (2012). *Theory of viscoelasticity: an introduction*. Elsevier.
- Craiem, D., Rojo, F. J., Atienza, J. M., Armentano, R. L., & Guinea, G. V. (2008). Fractional-order viscoelasticity applied to describe uniaxial stress relaxation of human arteries. *Physics in Medicine & Biology*, 53(17), 4543.
- Demirci, N., & Tönük, E. (2014). Non-integer viscoelastic constitutive law to model soft biological tissues to in-vivo indentation. *Acta of bioengineering and biomechanics*, 16(4).

- Doehring, T. C., Freed, A. D., Carew, E. O., & Vesely, I. (2005). Fractional order viscoelasticity of the aortic valve cusp: an alternative to quasilinear viscoelasticity. *Journal of biomechanical engineering*, 127(4), 700-708.
- Enelund, M., Mähler, L., Runesson, K., & Josefson, B. L. (1999). Formulation and integration of the standard linear viscoelastic solid with fractional order rate laws. *International Journal of Solids and Structures*, 36(16), 2417-2442.
- Freed, A. D., & Diethelm, K. (2006). Fractional calculus in biomechanics: a 3D viscoelastic model using regularized fractional derivative kernels with application to the human calcaneal fat pad. *Biomechanics and modeling in mechanobiology*, 5(4), 203-215.
- Fukunaga, M., & Shimizu, N. (2015). Fractional derivative constitutive models for finite deformation of viscoelastic materials. *Journal of Computational and Nonlinear Dynamics*, 10(6), 061002.
- Fung, Y. C. (1967). Elasticity of soft tissues in simple elongation. *American Journal of Physiology-Legacy Content*, 213(6), 1532-1544.
- Fung, Y. C. (1993). *Mechanical properties of living tissues* (Vol. 547). New York: Springer.
- Fung, Y. C., (1996) "Biomechanics Mechanical Properties of Soft Tissues: second edition," Springer-Verlag.
- Fung, Y. C., Tong, P., & Chen, X. (2017). *Classical and computational solid mechanics* (Vol. 2). World Scientific Publishing Company.
- Gemant, A. (1936). A method of analyzing experimental results obtained from elasto-viscous bodies. *Physics*, 7(8), 311-317.
- Gerasimov, A. N. (1948). A generalization of linear laws of deformation and its application to problems of internal friction. *Akad. Nauk SSSR. Prikl. Mat. Meh*, 12, 251-260.
- James, A. G., Green, A., & Simpson, G. M. (1975). Strain energy functions of rubber. I. Characterization of gum vulcanizates. *Journal of Applied Polymer Science*, 19(7), 2033-2058.
- Johnson, G. A., Tramaglino, D. M., Levine, R. E., Ohno, K., Choi, N. Y., & L-Y. Woo, S. (1994). Tensile and viscoelastic properties of human patellar tendon. *Journal of Orthopaedic Research*, 12(6), 796-803.

- Kaye, A. (1962). *Non-Newtonian flow in incompressible fluids*. College of Aeronautics Cranfield.
- Koeller, R. C. (1984). Applications of fractional calculus to the theory of viscoelasticity. *Journal of applied mechanics*, 51(2), 299-307.
- Lakes, R. S. (1998). *Viscoelastic solids* (Vol. 9). CRC press.
- Larrabee Jr, W. F. (1986). A finite element model of skin deformation. I. Biomechanics of skin and soft tissue: A review. *The Laryngoscope*, 96(4), 399-405.
- Liu, C. H., & Choudhry, S. (2004). Finite element analysis of hyperelastic material with MSC. Marc. *Computational mechanics*.
- Love, A. E. H. (2013). *A treatise on the mathematical theory of elasticity*. Cambridge university press.
- Loverro, A. (2004). Fractional calculus: history, definitions and applications for the engineer. *Rapport technique, Univeristy of Notre Dame: Department of Aerospace and Mechanical Engineering*, 1-28.
- Malkus, D. S., & Hughes, T. J. (1978). Mixed finite element methods—reduced and selective integration techniques: a unification of concepts. *Computer Methods in Applied Mechanics and Engineering*, 15(1), 63-81.
- Malvern, L. E. (1969). *Introduction to the Mechanics of a Continuous Medium* (No. Monograph).
- Mihai, L. A., & Goriely, A. (2017). How to characterize a nonlinear elastic material? A review on nonlinear constitutive parameters in isotropic finite elasticity. *Proceedings of the Royal Society A: Mathematical, Physical and Engineering Sciences*, 473(2207), 20170607.
- Miller-Young, J. E., Duncan, N. A., & Baroud, G. (2002). Material properties of the human calcaneal fat pad in compression: experiment and theory. *Journal of biomechanics*, 35(12), 1523-1531.
- Mino, G. D., Airey, G., Di Paola, M., Pinnola, F. P., D'Angelo, G., & Presti, D. L. (2016). Linear and nonlinear fractional hereditary constitutive laws of asphalt mixtures. *Journal of Civil Engineering and Management*, 22(7), 882-889.
- Mooney, M. (1940). A theory of large elastic deformation. *Journal of applied physics*, 11(9), 582-592.

- Nutting, P. G. (1921). A new general law of deformation. *Journal of the Franklin Institute*, 191(5), 679-685.
- Ogden, R. W. (1972). Large deformation isotropic elasticity—on the correlation of theory and experiment for incompressible rubberlike solids. *Proceedings of the Royal Society of London. A. Mathematical and Physical Sciences*, 326(1567), 565-584.
- Ogden, R. W. (1997). *Non-linear elastic deformations*. Courier Corporation.
- Petekkaya, A. T., & Tonuk, E. (2011). In vivo indenter experiments via ellipsoid indenter tips to determine the personal and local in-plane anisotropic mechanical behavior of soft biological tissues. *JOURNAL OF THE FACULTY OF ENGINEERING AND ARCHITECTURE OF GAZI UNIVERSITY*, 26(1), 63-72.
- Podlubny, I. (1998). *Fractional differential equations: an introduction to fractional derivatives, fractional differential equations, to methods of their solution and some of their applications* (Vol. 198). Elsevier.
- Podlubny, I. (2012). *Matlab Central*. <https://www.mathworks.com/matlabcentral/fileexchange/8738-mittag-leffler-function>.
- Rabotnov, Y. (2014). Equilibrium of an elastic medium with after-effect. *Fractional Calculus and Applied Analysis*, 17(3), 684-696.
- Rivlin, R. S. (1947). Torsion of a rubber cylinder. *Journal of Applied Physics*, 18(5), 444-449.
- Rivlin, R. S. (1965). Nonlinear viscoelastic solids. *Siam Review*, 7(3), 323-340.
- Schiessel, H., Metzler, R., Blumen, A., & Nonnenmacher, T. F. (1995). Generalized viscoelastic models: their fractional equations with solutions. *Journal of physics A: Mathematical and General*, 28(23), 6567.
- Schmidt, A., & Gaul, L. (2002). Finite element formulation of viscoelastic constitutive equations using fractional time derivatives. *Nonlinear Dynamics*, 29(1-4), 37-55.
- Soczkiwicz, E. (2002). Application of fractional calculus in the theory of viscoelasticity. *Molecular and Quantum Acoustics*, 23, 397-404.
- Timoshenko, S. (1983). *History of strength of materials: with a brief account of the history of theory of elasticity and theory of structures*. Courier Corporation.

- Tönük, E., & Silver-Thorn, M. B. (2004). Nonlinear viscoelastic material property estimation of lower extremity residual limb tissues. *Journal of biomechanical engineering*, 126(2), 289-300.
- Torvik, P. J., & Bagley, R. L. (1984). On the appearance of the fractional derivative in the behavior of real materials. *Journal of Applied Mechanics*, 51(2), 294-298.
- Treloar, L. R. G. (1975). *The physics of rubber elasticity*. Oxford University Press, USA.
- Tschoegl N W (1989) *The Phenomenological Theory of Linear Viscoelastic Behavior* (Berlin: Springer)
- Ward I M (1983) *Mechanical Properties of Solid Polymers* (Chichester: Wiley)